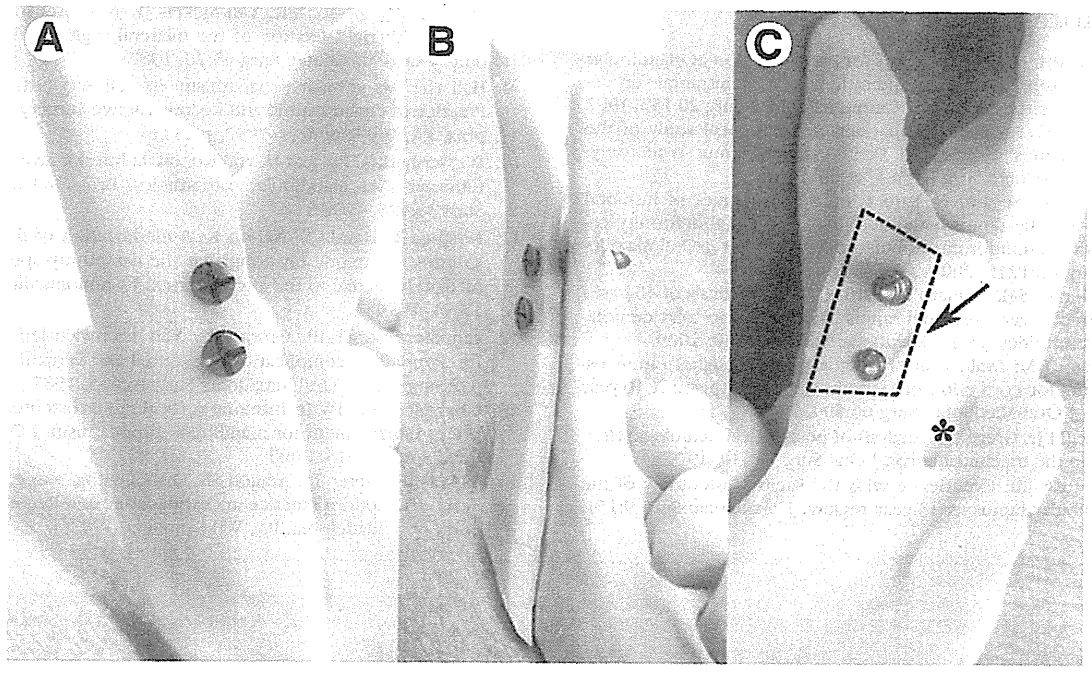

FIGURE 3. Rigid fixation of intraoral vertico-sagittal ramus osteotomy using a mandibular model. *A,* Lateral and *B,* anterior views of the left mandibular ramus. Screws can be inserted into the subcoronoid area on the distal segment and the subcondylar area on the proximal segment. *C,* Medial view showing a relatively large area for screw insertion (*dashed rectangular area*). *Arrow* indicates lingular of mandible. *Asterisk* indicates mandibular foramen.

Fujimura and Bessho. Rigid Fixation of IVSRO. J Oral Maxillofac Surg 2012.

Discussion

The main advantage of rigid fixation IVSRO over SSRO in treating prognathism, when the posterior margin of the ramus curves inward or the ramus is thin, may be the decreased risk of postoperative NSD. The incidence of long-term NSD of the lower lip and chin in IVSRO was 0% to 6%[1,4,5] compared with 39% to 85% for SSRO.[6-10] Although the osteotomy plane is between the mandibular canal and the lateral cortical plate of the ramus, as in SSRO, damage to the IAN can be avoided because the osteotomy is performed from a point in front of the foramen between the mandibular canal and the immediately medial lateral cortical bone,[1,11] making it likely to strip the lateral cortical bone from the bone marrow. Although a low incidence of NSD is also observed with IVRO,[9,12] rigid fixation with screws or bone plates has several disadvantages, including technical difficulty[9,13] and rotation of the condyle to the lateral side.[1] IVSRO is distinguished by flat and larger contact areas of segments and more favorable healing of the medulla to the cortex than the cortex-to-cortex healing of IVRO.[1]

In SSRO, the excess overlap of the anterior edge of the proximal segment must be removed to fit the 2 segments and/or prevent distal rotation of the proximal segment.[1,4] In IVSRO, there is no excess overlap of the proximal segment.

It is easy to check the position of the distal segment after osteotomy because the anterior area of the proximal segment is removed beforehand; hence, the subcoronoid area of the distal segment and the subcondylar area of the proximal segment can be used for insertion of screws. The area available for screw insertion is relatively large and the ends of the inserted screws may be viewed at the medial aspect of the distal segment because, at the internal oblique ridge, the bone thickness of this subcoronoid area in the distal segment is relatively thin compared with the retromolar areas as in SSRO. Therefore, in many patients, a 90° angle screwdriver system with 12-mm screw length can be used without drilling through a trocar inserted through the skin (Fig 3A–C).

When planning rigid fixation using IVSRO, the following 2 conditions are preferable: *1)* mandibular setback (about ≥5 mm) and *2)* counterclockwise rotation. Because this osteotomy procedure has a large contact area between the proximal and distal segments, compared with IVRO, the segments are usually fixed with screws in only the setback side for horizontal rotation for mandibular asymmetry (Fig 2C).

Additional studies including the development of osteotomy instruments and drilling systems to simplify the surgical procedure of IVSRO are needed to validate the advantages of this procedure.

References

1. Choung PH: A new osteotomy for the correction of mandibular prognathism: Techniques and rationale of the intraoral vertico-sagittal ramus osteotomy. J Craniomaxillofac Surg 20:153, 1992
2. Fujimura K, Segami N, Kobayashi S: Anatomical study of the complications of intraoral vertico-sagittal ramus osteotomy. J Oral Maxillofac Surg 64:384, 2006
3. Fujimura K, Segami N, Sato J, et al: Advantages of intraoral verticosagittal ramus osteotomy in skeletofacial deformity patients with temporomandibular joint disorders. J Oral Maxillofac Surg 62:1246, 2004
4. Lima Júnior SM, Granato R, Marin C, et al: Analysis of 40 cases of intraoral verticosagittal ramus osteotomies to treat dentofacial deformities. J Oral Maxillofac Surg 67:1840, 2009
5. Hashemi HM: Evaluation of intraoral verticosagittal ramus osteotomy for correction of mandibular prognathism: A 10-year study. J Oral Maxillofac Surg 66:509, 2008
6. Walter JM Jr, Gregg JM: Analysis of postsurgical neurologic alteration in the trigeminal nerve. J Oral Surg 37:410, 1979
7. MacIntosh RB: Experience with the sagittal osteotomy of the mandibular ramus: A 13-year review. J Maxillofac Surg 9:151, 1981
8. Nishioka GJ, Zysset MK, Van Sickels JE: Neurosensory disturbance with rigid fixation of the bilateral sagittal split osteotomy. J Oral Maxillofac Surg 45:20, 1987
9. Hall HD: Mandibular prognathism, *in* Bell WH (ed): Modern Practice in Orthognathic and Reconstructive Surgery. Philadelphia, PA, WB Saunders, 1992, p 2111
10. Westermark A, Bystedt H, von Konow L: Inferior alveolar nerve function after mandibular osteotomies. Br J Oral Maxillofac Surg 36:425, 1998
11. Kitajima T, Handa Y, Naitoh K: A modification of the sagittal splitting technique ensuring that the osteotomy split lies immediately medial to the lateral cortex. J Craniomaxillofac Surg 17:53, 1989
12. van Merkesteyn JP, Groot RH, Van Leeuwaarden R, et al: Intra-operative complications in sagittal and vertical ramus osteotomies. Int J Oral Maxillofac Surg 16:665, 1987
13. Ghali GE, Sikes JW Jr: Intraoral vertical ramus osteotomy as the preferred treatment for mandibular prognathism. J Oral Maxillofac Surg 58:313, 2000
14. Sickels JEV, Jeter TS, Aragon SB: Orthognathic surgery, *in* Bell WH (ed): Modern Practice in Orthognathic and Reconstructive Surgery. Philadelphia, PA, WB Saunders, 1992, p 1980

ADVANCED MATERIALS
www.advmat.de

Innovative Collagen Nano-Hydroxyapatite Scaffolds Offer a Highly Efficient Non-Viral Gene Delivery Platform for Stem Cell-Mediated Bone Formation

*Caroline M. Curtin, Gráinne M. Cunniffe, Frank G. Lyons, Kazuhisa Bessho, Glenn R. Dickson, Garry P. Duffy, and Fergal J. O'Brien**

Treatments combining nanotechnology with gene and stem cell-based therapies are increasingly showing potential in the field of tissue engineering. In this study, we describe the development of a bioactive and biodegradable collagen nano-hydroxyapatite (coll-nHA) scaffold with the capacity to be used as a gene delivery platform to promote transfection of mesenchymal stem cells (MSCs). Firstly, a nano-hydroxyapatite (nHA) synthesis technique was optimized, and the ability of the nHA particles to act as non-viral vectors for delivery of plasmid-DNA (pDNA) encoding bone morphogenetic protein 2 (BMP2), a gene capable of stimulating MSCs along the osteogenic lineage,[1] was determined. The nHA particles were then combined with collagen scaffolds, with an architecture previously optimized in our laboratory for bone repair, to yield highly porous, mechanically stable, osteoconductive and osteoinductive coll-nHA scaffolds. The ability of this scaffold to act as a gene-activated matrix (GAM) for BMP2 delivery was demonstrated with successful transfection of MSCs resulting in high levels of calcium production.

Commonly, viruses including adenovirus and lentivirus have been used as gene delivery vectors to efficiently transfer a gene of interest to the host genome.[2,3] However, using viral vector-based technology possesses numerous disadvantages not least the known safety concerns associated with insertational mutagenesis following viral integration[4] and the adverse immune responses observed in patients.[5] Additional problems include the time consuming and labour intensive process involved in the production of such viruses, thereby limiting their potential for tissue engineering.

Therefore, we sought to develop a safe and effective non-viral based gene delivery vector to overcome the associated viral vector safety problems while being amenable to cost-effective mass production. Typically however, non-viral transfection methods have demonstrated lower efficiencies than that of their viral counterparts[6] but have an enhanced safety profile. Lipid and polymer-based gene delivery vectors are the most common and efficient non-viral delivery methods utilised but these are often associated with significant cytotoxicity thereby reducing their clinical relevance.[7] To overcome this cytotoxic issue, we have developed non-aggregating nHA particles[8] for gene delivery.

Calcium phosphate has long been used as a method of DNA transfection in various cell lines.[9] As hydroxyapatite is a calcium phosphate mineral, it possesses many advantages for use as a gene delivery vector. nHA particles are biocompatible[10] and bioresorbable, non-toxic and cost effective to produce, and they exhibit a high binding affinity for DNA most likely due to interactions between calcium ions in the apatite and the negatively charged phosphate groups in DNA.[11] A nHA synthesis method has been developed within our laboratory to yield homogenous non-aggregating particles <200 nm in size.[8] Following extensive testing to demonstrate their ability to act as gene delivery vectors when combined with MSCs, the nHA particles were investigated as BMP2 carriers in 2D osteogenic culture and additionally in the 3D environment of collagen-based scaffolds. BMP2 was assessed due to its known therapeutic capacity for bone repair.[1,12,13]

In addition to using the nHA particles as gene delivery vectors, they were also used to develop an innovative coll-nHA scaffold. The nHA particles were combined with highly porous collagen-based scaffolds developed within our laboratory, with a structure optimized for bone repair,[14–17] to yield highly biocompatible, mechanically superior, osteoconductive and osteoinductive coll-nHA scaffolds.[18] Finally, we assessed the capacity of our 3D coll-nHA scaffolds to act as GAMs. We evaluated whether the subsequent culture of MSCs on the collagen and coll-nHA scaffolds containing nHA-BMP2 particles results in conditions sufficient to promote and enhance *in vitro* osteogenesis compared to non-transfected MSCs on these scaffolds.

Firstly, we performed optimization experiments to yield the most effective nHA particles for successful cellular transfection (Supporting Information). The transfection efficiency of nHA

Dr. C. M. Curtin, Dr. F. G. Lyons, Dr. G. P. Duffy, Prof. F. J. O'Brien
Department of Anatomy
Royal College of Surgeons in Ireland, Dublin, Ireland
E-mail: fjobrien@rcsi.ie
Dr. C. M. Curtin, Dr. G. M. Cunniffe, Dr. G. P. Duffy, Prof. F. J. O'Brien
Trinity Centre for Bioengineering
Trinity College Dublin, Ireland
Prof. K. Bessho
Department of Oral & Maxillofacial Surgery
Graduate School of Medicine
Kyoto University, Japan
Dr. G. R. Dickson
Centre for Cancer Research and Cell Biology
School of Medicine
Dentistry and Biomedical Sciences
Queen's University Belfast, Northern Ireland

DOI: 10.1002/adma.201103828

COMMUNICATION

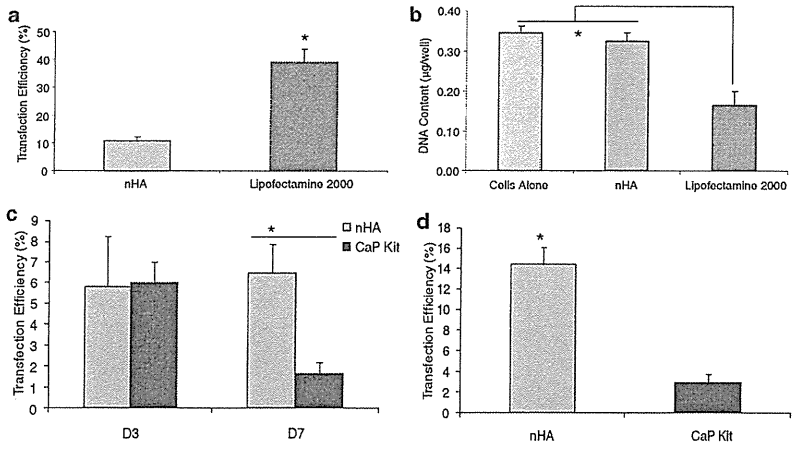

Figure 1. Nano-hydroxyapatite particle transfection efficiency and cell viability analysis. Quantification of GFP expression by FACS analysis revealed enhanced transfection efficiency with the positive control, Lipofectamine 2000, compared to nHA particles (a). Upon quantification of DNA content, there was a significant decrease in Lipofectamine 2000-pLuc transfected cells compared to nHA-pLuc transfected cells and cells alone (b). When nHA-GFP transfection efficiency was compared to a commercial CaP kit, quantification of GFP expression demonstrated a significant increase following nHA transfection by day 7 (c). Quantification of GFP expression in transfected hMSCs at day 3 also demonstrated a significant increase in transfection efficiency using 5 µg plasmid DNA compared to the commercial CaP kit (d). Error bars represent standard error of the mean (n = 3). * $P \leq 0.05$.

particle transfection was determined to be ~12% compared to ~40% for Lipofectamine 2000 transfection using green fluorescent protein (GFP) pDNA (**Figure 1**a). Following quantification of DNA content to assess proliferation, nHA-luciferase (nHA-pLuc) transfected rat MSCs (rMSCs) demonstrated similar DNA content levels to non-transfected cells while a significant decrease was observed in Lipofectamine 2000-pLuc transfected rMSCs indicating a potent cytotoxic effect using this transfection method (Figure 1b). The transfection efficiency obtained using these nHA particles was also compared to a commercially available calcium phosphate (CaP) transfection kit. MSCs transfected with nHA revealed a significant increase in GFP expression at day 7 compared to those transfected with the commercial CaP kit (Figure 1c). Furthermore, when transfection using the nHA particles was translated from rat to human MSCs (hMSCs) and compared to the CaP transfection kit, even greater levels of transfection were obtained than that following rMSC transfection at the same pDNA concentrations (Figure 1d). Interestingly, transfection using the nHA particles was also more efficient in hMSCs compared to rMSCs. This study thus demonstrates the superior capacity of these novel nHA particles to act as efficient non-viral delivery vectors for MSC transfection compared to other commercially available transfection delivery vectors and their potential for use in clinical applications with human cells.

Having demonstrated the ability of these nHA particles to act as competent gene delivery agents, the osteogenic ability of rMSCs following nHA-BMP2 transfection was assessed in monolayer using two different concentrations of BMP2: 1 µg and 3 µg. Alizarin red staining revealed enhanced calcium deposition within the nHA-BMP2 rMSCs compared to rMSCs alone and nHA-pDNA-free rMSC controls (**Figure 2**a). Similarly, von Kossa staining displayed a comparable trend with nHA-BMP2 rMSCs demonstrating enhanced phosphate deposition compared to controls (Figure 2b). Quantification of calcium deposition corroborated the staining results, showing a significant increase in calcium deposition within the nHA-BMP2 transfected cells compared to the controls (Figure 2c). As both BMP2 concentrations resulted in equivalent calcium content, this indicates the nHA particles are providing an efficient osteoinductive effect negating the requirement for high levels of BMP2 to induce the enhanced osteogenic response.

The final stage of the study assessed the potential of coll-nHA and nHA-free collagen alone scaffolds to act as GAMs using the nHA particle transfection technique and compared to Lipofectamine 2000 (Supporting Information). The osteogenic potential of MSCs on coll-nHA scaffolds was assessed and compared to collagen alone scaffolds following nHA-BMP2 particle transfection. Results obtained were significant in two ways. Firstly, alizarin red (**Figure 3**a) and von Kossa staining (Supporting Information) revealed enhanced staining on the coll-nHA scaffolds compared to the collagen scaffolds in all treatment groups indicating the improved osteogenic properties of these scaffolds due to the osteoinductive and osteoconductive nature of the nHA particles. Further enhanced staining was then observed within both scaffold types following nHA-BMP2 transfection compared to the rMSCs alone and nHA-pDNA-free rMSC groups demonstrating the potent ability of the nHA particles to act as efficient gene delivery vectors when combined with both scaffold types. In addition, osteocalcin expression, indicative of differentiation into an osteoblastic phenotype, was enhanced in the coll-nHA nHA-BMP2 group over all other groups evaluated, (Figure 3b), supporting alizarin red and Von Kossa staining. When calcium deposition was assessed, the highest levels were observed within the coll-nHA scaffolds demonstrating their superior ability to act as efficient gene delivery platforms (Figure 3c).

In conclusion, this study describes the development of a safe and effective non-viral gene delivery vector that overcomes the common viral-based gene delivery vector safety problems. We demonstrated the superior capacity of these novel non-aggregating nHA particles to act as efficient non-viral delivery vectors for rMSC and hMSC transfection compared to other commercially available sources. Incorporation of these nHA particles combined with pDNA in collagen-based scaffolds resulted in the development of a therapeutic GAM. Enhanced osteogenesis was then observed following nHA-BMP2 transfection in both 2D and 3D cultures when using low levels of pBMP2 demonstrating their innate capacity for promoting bone formation. When nHA-BMP2 particles were combined with the additional osteoinductive and osteoconductive nature of coll-nHA scaffolds, the inherent bone forming capacity was considerably enhanced. From a general tissue engineering perspective, the results demonstrate the promise of these coll-nHA scaffolds

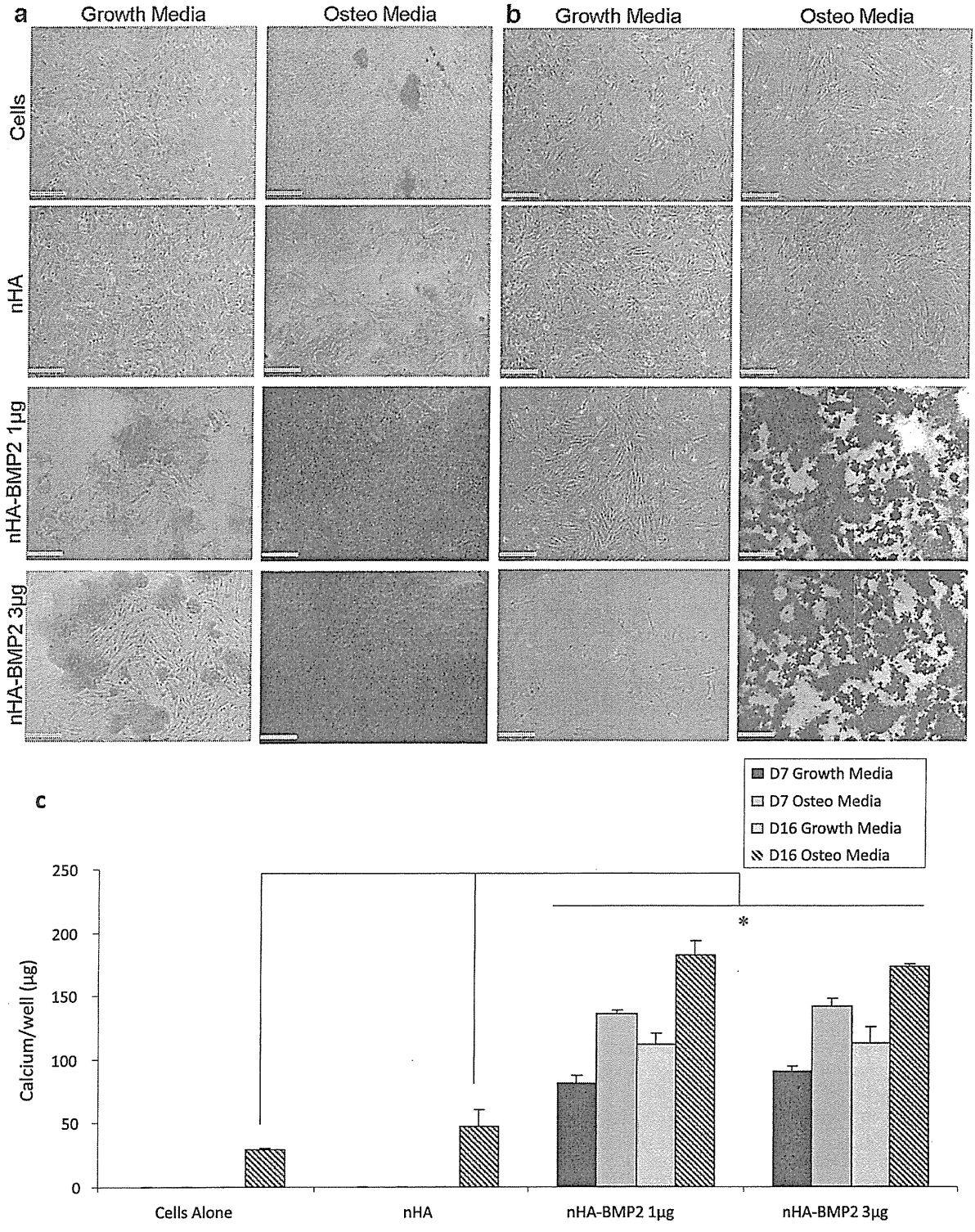

Figure 2. Enhanced 2D osteogenesis following nHA-BMP2 transfection. Brightfield images of alizarin red (a) and von Kossa (b) stained cells demonstrated enhanced staining in nHA-BMP2 treatment groups (growth and osteogenic media treated) compared to the cells alone treatment group. Magnification bar = 200 µm. Similarly, calcium quantification demonstrated a dose dependent increase in calcium levels in both nHA-BMP2 transfected growth and osteogenic media treated cells at days 7 and 16 (c). Error bars represent standard error of the mean (n = 3). * $P \leq 0.05$ compared to cells alone.

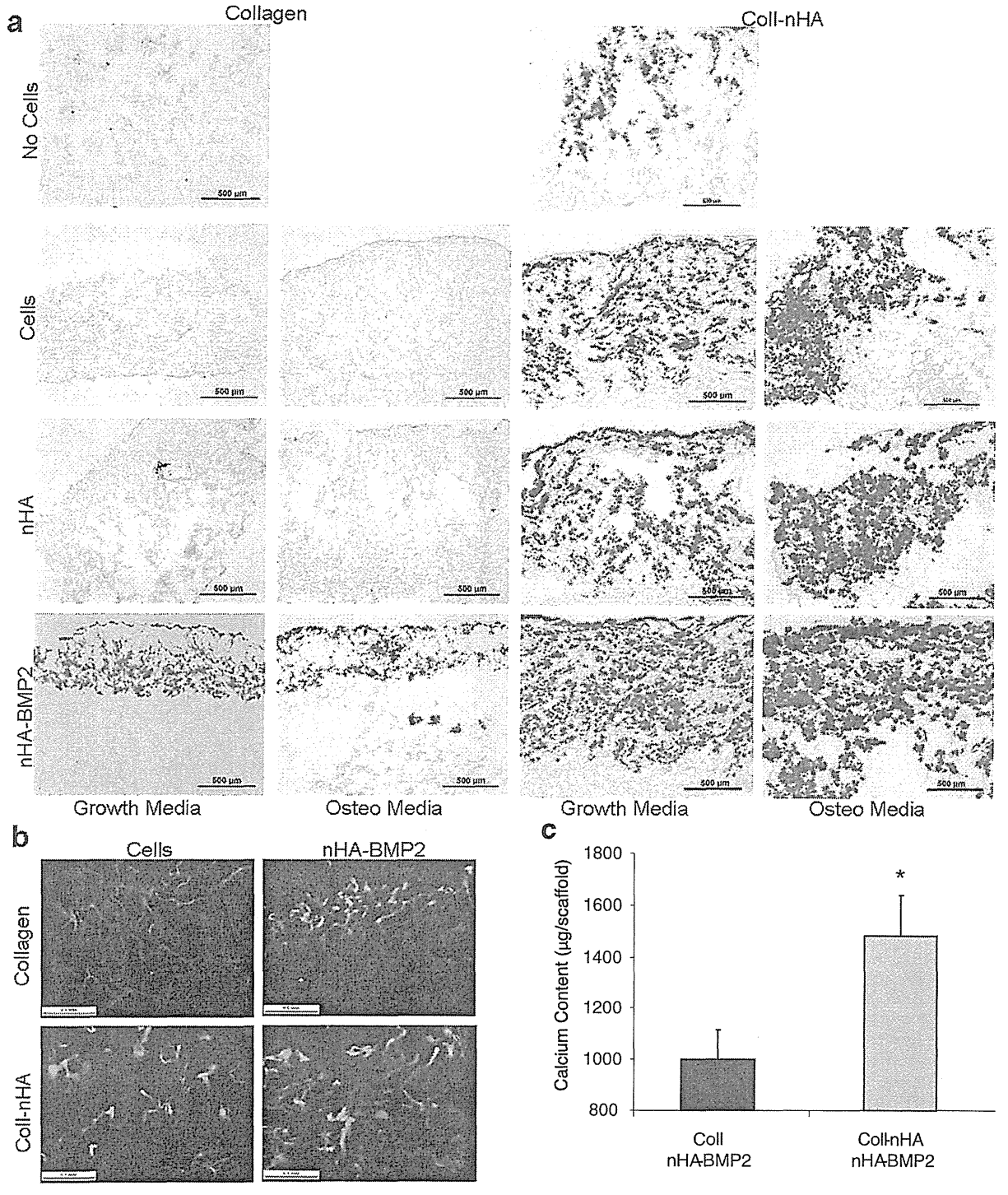

Figure 3. Enhanced 3D osteogenesis following nHA-BMP2 transfection. Alizarin red staining revealed enhanced calcium deposition on coll-nHA scaffolds under all treatments evaluated compared to collagen alone scaffolds (a). Most intense staining was observed on coll-nHA scaffolds with nHA-BMP2 transfection following osteogenic media treatment. Magnification bar = 500 µm. Osteocalcin immunofluorescence corroborates alizarin red staining demonstrating enhanced expression within the coll-nHA nHA-BMP2 scaffold compared to the cells alone and collagen nHA-BMP2 scaffold following osteogenic media treatment (b). Magnification bar = 100 µm. Calcium quantification of nHA-BMP2 transfected scaffolds demonstrated a significant increase in calcium content on coll-nHA scaffolds (c). Error bars represent standard error of the mean (n = 3). * $P \leq 0.05$ compared to the collagen nHA-BMP2 scaffold.

as effective gene delivery platforms and thus demonstrate their potential as superior alternatives to existing bone graft treatments.

Experimental Section

nHA particle synthesis optimization and nHA-pDNA complex preparation: nHA particles were precipitated as previously described.[8] The phosphate solution was prepared in the presence or absence of Darvan dispersing agent–no Darvan (0% v/v Darvan), low Darvan (0.017% v/v Darvan), and high Darvan (0.1% v/v Darvan) to determine the effect of Darvan addition on transfection efficiency. Filtered (0.2 μm filters) nHA solution (150 μl) was then added to 3 μg pDNA and 6.25 μl 250 mM $CaCl_2$ for transfection with a final volume of 150 μl nHA-pDNA suspension added per well in 12 well plates.

A Quant-iT PicoGreen dsDNA kit (Invitrogen) was used according to the manufacturer's protocol to determine the pDNA binding efficiency of nHA particles synthesized with and without Darvan. This kit was also used to assess DNA content following GFP transfection. Particle size distributions were measured using dynamic light scattering (DLS; ZetaSizer 3000 HS, Malvern Instruments). Zeta Potential (ZP) readings (n = 6) were conducted on freshly prepared suspensions using a ZetaSizer 3000 HS (Malvern instruments) to determine stability of nHA particles within the solution.

Plasmid propagation: pMaxGFP (Amaxa, Lonza), pGaussian-Luciferase (pLuc; New England Biolabs) and pBMP2,[19] encoding the reporter genes, green fluorescent protein (GFP), luciferase and bone morphogenetic protein 2 (BMP2) respectively were used in this study. Plasmid amplification was carried out by transforming One Shot® TOP10 Chemically Competent *E. coli* bacterial cells according to the manufacturer's protocol and the pDNA was collected using Maxiprep kits (Qiagen).

Cell culture: rMSCs were isolated from the femora and tibiae of male Wistar rats with ethical approval (REC 237) from the Research Ethical Committee, Royal College of Surgeons in Ireland, Dublin. Cells were then expanded in culture by direct plating and cultured under normal growth conditions at 37 °C in 5% CO_2 in standard rMSC growth medium (Dulbecco's Minimum Essential Medium) supplemented with 2% penicillin/streptomycin, 1% L-glutamine, 1% GlutaMAX, 1% non-essential amino acids and 10% foetal bovine serum (FBS; BioSera). hMSCs were obtained as a kind gift from the Regenerative Medicine Institute (REMEDI), NUI Galway, Ireland. All procedures were performed with informed donor consent and ethically approved by the Clinical Research Ethical Committee at University College Hospital, Galway. Cells were cultured under normal growth conditions at 37 °C in 5% CO_2 in standard hMSC growth medium (Dulbecco's Minimum Essential Medium supplemented with 2% penicillin/streptomycin and 10% FBS).

2D transfection study: MSCs were plated in 12 well plates at a density of 5×10^4 cells/well. Media was changed 24 hrs after plating, and 1 hr before transfections were conducted, media was replaced. The commercial lipid transfection agent Lipofectamine 2000 (Invitrogen) was used as a positive control, according to the manufacturer's protocol. The prepared nHA/Lipofectamine:pDNA complex solutions (150 μl) were added to the wells and incubated for 15 mins before growth media was added. OptiMEM reduced-serum media was required for the Lipofectamine 2000 transfected cells, and this solution was removed 6 hrs after transfection and replaced with regular growth media. Cells were assessed for transgene expression on day 3 post-transfection using fluorescence microscopy and days 3 and 7 using flow cytometry (BD FACSCanto II, BD Biosciences). A Live/Dead Viability/Cytotoxicity kit (Invitrogen) was used for calcein staining of the rMSCs to identify live cells according to the manufacturer's protocol. The nHA particles were also compared to a CaP transfection kit (Sigma) to determine transfection capabilities at day 3 (hMSCs and rMSCs) and day 7 (rMSCs). Equal pDNA levels (5 μg) were assessed and transfection was performed according to the manufacturer's protocol.

Scaffold fabrication: Collagen and collagen nHA (coll-nHA) scaffolds investigated in this study were manufactured using a technique developed in our laboratory.[14–18] For the coll-nHA scaffolds, nHA particles were synthesized as previously described and added to the collagen slurry during the blending process. A nHA suspension was added to the collagen slurry yielding a 1:1 scaffold of nHA:collagen. Slurries were freeze-dried and scaffolds were cross-linked and sterilized using a dehydrothermal (DHT) treatment.[20] Cylindrical scaffolds (9.5 mm diameter, 4 mm height) were further cross-linked with 14 mM N-(3-Dimethylaminopropyl)-N′-ethylcarbodiimide hydrochloride (EDAC) and 5.5 mM N-hydroxysuccinimide (NHS) in dH_2O.[21]

3D transfection study: The pDNA-complexes were added to scaffolds by soak loading 75 μl of the pDNA-complex solution drop-wise onto each side of the scaffold surface with a 15 min incubation step between additions. Scaffold samples were then seeded with 2.5×10^5 rMSCs on each side of the scaffold including a 15 min incubation step between additions. Constructs were cultured in growth media for 24 hrs before being replaced with either growth media for transgene expression profile experiments or osteogenic media (growth media with ascorbic acid (50 μg/ml), β-glycerophosphate (10 mM) and dexamethasone (100 nM)) for osteogenesis experiments. Constructs were cultured under standard conditions (37 °C, 5% CO_2), and the media was replenished every 3–4 days up to 35 days. Constructs (n = 3) were analysed for calcium content or constructs (n = 1) were fixed in 10% formalin for processing prior to histological analysis.

Luciferase assay: A LumiFlex GLuc assay (New England Biolabs) was used to quantify the expression of luciferase in media samples from pLuc-transfected MSC seeded constructs according to the manufacturer's protocol.

Calcium quantification: Quantification of calcium deposition within 2D and 3D osteogenesis experiments was performed using the Calcium Liquicolor kit (Stanbio Laboratories) according to the manufacturer's protocol.

Mineralization: Wax embedded scaffold sections (10 μm) were stained with either Von Kossa or alizarin red to evaluate cell-mediated matrix deposition and mineralization within the scaffolds according to standard protocols.

Immunofluorescence: Wax embedded scaffold sections (10 μm) were permeabilized with 0.1% Triton-X100 for 10 mins and blocked with 0.1% Triton-X100/2% bovine serum albumin in phosphate buffered saline (PBS) for 2 hrs at room temperature. Cells were incubated with osteocalcin (1:50) at 4 °C overnight, washed three times with PBS, then incubated with secondary antibody (1:200) for 1 h at room temperature in the dark and washed as before, prior to coverslipping.

Statistical analysis: Results are expressed as mean ± standard deviation. Two-way analysis of variance (ANOVA) followed by a pair wise multiple comparison procedure (Tukey test) was used. Statistical significance was declared at $p \leq 0.05$.

Supporting Information

Supporting Information is available from the Wiley Online Library or from the author.

Acknowledgements

This work was supported by the European Research Council under the European Community's Seventh Framework Programme (FP7/2007-2013)/ERC grant agreement n° 239685 and Science Foundation Ireland, President of Ireland Young Researcher Award (04/Yl1/B531). Collagen was provided by Integra LifeSciences Corporation. hMSCs were a kind gift from Prof. Frank Barry, Dr. Mary Murphy and Georgina Shaw, REMEDI, NUI Galway, Ireland.

Received: October 4, 2011
Revised: November 29, 2011
Published online: January 2, 2012

[1] C. M. Edgar, V. Chakravarthy, G. Barnes, S. Kakar, L. C. Gerstenfeld, T. A. Einhorn, *Bone.* **2007**, *40*, 1389–1398.
[2] A. Ishihara, L. J. Zekas, S. E. Weisbrode, A. L. Bertone, *Gene Ther.* **2010**, *17*, 733–744.
[3] A. Van Damme, L. Thorrez, L. Ma, H. Vandenburgh, J. Eyckmans, F. Dell'Accio, C. De Bari, F. Luyten, D. Lillicrap, D. Collen, T. Vanden-Driessche, M. K. Chuah, *Stem Cells.* **2006**, *24*, 896–907.
[4] Y. Shou, Z. Ma, T. Lu, B. P. Sorrentino, *Proc. Natl. Acad. Sci. USA* **2006**, *103*, 11730–11735.
[5] S. Hacein-Bey-Abina, C. von Kalle, M. Schmidt, F. Le Deist, N. Wulffraat, E. McIntyre, I. Radford, J. L. Villeval, C. C. Fraser, M. Cavazzana-Calvo, A. Fischer, *N Engl. J. Med.* **2003**, *348*, 255–256.
[6] C. Pichon, L. Billiet, P. Midoux, *Curr. Opin. Biotechnol.* **2010**, *21*, 640–645.
[7] S. D. Patil, D. G. Rhodes, D. J. Burgess, *AAPS J.* **2005**, *7*, E61–77.
[8] G. M. Cunniffe, F. J. O'Brien, S. Partap, T. J. Levingstone, K. T. Stanton, G. R. Dickson, *J. Biomed. Mater. Res. A.* **2010**, *95*, 1142–1149.
[9] D. Olton, J. Li, M. E. Wilson, T. Rogers, J. Close, L. Huang, P. N. Kumta, C. Sfeir, *Biomaterials.* **2007**, *28*, 1267–1279.
[10] M. Kester, Y. Heakal, T. Fox, A. Sharma, G. P. Robertson, T. T. Morgan, E. I. Altinoglu, A. Tabakovic, M. R. Parette, S. M. Rouse, V. Ruiz-Velasco, J. H. Adair, *Nano Lett.* **2008**, *8*, 4116–4121.
[11] M. Okazaki, Y. Yoshida, S. Yamaguchi, M. Kaneno, J. C. Elliott, *Biomaterials.* **2001**, *22*, 2459–2464.
[12] Y. Okubo, K. Bessho, K. Fujimura, S. Kaihara, T. Iizuka, S. Miyatake, *Life Sci.* **2001**, *70*, 325–336.
[13] S. Kaihara, K. Bessho, Y. Okubo, J. Sonobe, M. Kawai, T. Iizuka, *Gene Ther.* **2004**, *11*, 439–447.
[14] F. J. O'Brien, B. A. Harley, I. V. Yannas, L. Gibson, *Biomaterials.* **2004**, *25*, 1077–1086.
[15] F. J. O'Brien, B. A. Harley, I. V. Yannas, L. J. Gibson, *Biomaterials.* **2005**, *26*, 433–441.
[16] C. M. Murphy, M. G. Haugh, F. J. O'Brien, *Biomaterials.* **2010**, *31*, 461–466.
[17] F. G. Lyons, A. A. Al-Munajjed, S. M. Kieran, M. E. Toner, C. M. Murphy, G. P. Duffy, F. J. O'Brien, *Biomaterials.* **2010**, *31*, 9232–9243.
[18] G. M. Cunniffe, G. R. Dickson, S. Partap, K. T. Stanton, F. J. O'Brien, *J. Mater. Sci. Mater. Med.* **2010**, *21*, 2293–2298.
[19] M. Kawai, K. Bessho, S. Kaihara, J. Sonobe, K. Oda, T. Iizuka, H. Maruyama, *Hum. Gene Ther.* **2003**, *14*, 1547–1556.
[20] M. G. Haugh, M. J. Jaasma, F. J. O'Brien, *J. Biome. Mater. Res. Part A.* **2009**, *89A*, 363–369.
[21] M. G. Haugh, C. M. Murphy, R. C. McKiernan, C. Altenbuchner, F. J. O'Brien, *Tissue Eng. Part A* **2011**, *17*, 1201–1208.

STEM CELLS AND DEVELOPMENT
Volume 22, Number 1, 2013

DOI: 10.1089/scd.2012.0127

Human Induced Pluripotent Stem Cells Differentiated into Chondrogenic Lineage *Via* Generation of Mesenchymal Progenitor Cells

Noriaki Koyama,[1,2] Masako Miura,[1] Kazumasa Nakao,[2] Eri Kondo,[1] Toshihito Fujii,[1] Daisuke Taura,[1] Naotetsu Kanamoto,[1] Masakatsu Sone,[1] Akihiro Yasoda,[1] Hiroshi Arai,[1] Kazuhisa Bessho,[2] and Kazuwa Nakao[1]

Human induced pluripotent stem cells (hiPSCs) exhibit pluripotency, proliferation capability, and gene expression similar to those of human embryonic stem cells (hESCs). hESCs readily form cartilaginous tissues in teratomas in vivo; despite extensive effort, however, to date no efficient method for inducing mature chondrocytes in vitro has been established. hiPSCs can also differentiate into cartilage in vivo by teratoma formation, but as with hESCs, no reliable system for in vitro chondrogenic differentiation of hiPSCs has yet been reported. Here, we examined the chondrogenic differentiation capability of hiPSCs using a multistep culture method consisting of embryoid body (EB) formation, cell outgrowth from EBs, monolayer culture of sprouted cells from EBs, and 3-dimensional pellet culture. In this culture process, the cell density of monolayer culture was critical for cell viability and subsequent differentiation capability. Monolayer-cultured cells exhibited fibroblast-like morphology and expressed markers for mesenchymal stem cells. After 2–3 weeks of pellet culture, cells in pellets exhibited a spherical morphology typical of chondrocytes and were surrounded by extracellular matrix that contained acidic proteoglycans. The expression of type II collagen and aggrecan in pellets progressively increased. Histological analysis revealed that over 70% of hiPSC-derived pellets successfully underwent chondrogenic differentiation. Using the same culture method, hESCs showed similar histological changes and gene expression, but differentiated slightly faster and more efficiently than hiPSCs. Our study demonstrates that hiPSCs can be efficiently differentiated into the chondrogenic lineage in vitro via generation of mesenchymal progenitor cells, using a simplified, multistep culture method.

Introduction

The increasing prevalence of degenerative cartilage diseases, particularly osteoarthritis, presents an important social and healthcare problem. Methods for regenerating chondrocytes and cartilage tissue are expected to transform conventional therapies for such diseases. Tissue regeneration approaches also hold promise for treating craniofacial deformities caused by congenital diseases, trauma, or surgical resection for malignancy that require reconstruction of cartilage/bone tissues for cosmetic and functional improvement. To date, cartilaginous tissue engineering research has focused largely on the use of mesenchymal stem cells (MSCs) and mature chondrocytes as resources. Indeed, bone marrow-derived MSCs (BMMSCs) are currently being tested in clinical trials for several orthopedic applications, including articular cartilage repair [1–3]. MSCs can be isolated from various postnatal tissues [4–8] and do not trigger an immunological reaction after transplantation. However, they possess limited proliferation capability and differentiation directions and decrease their differentiation potential with increasing donor age [9,10]. Moreover, the invasive procedure required to harvest MSCs presents another hurdle to widespread clinical application.

Human induced pluripotent stem cells (hiPSCs) have been generated from somatic cells by introducing Oct3/4 and Sox2 along with either Klf4 and c-Myc or Nanog and Lin28, using retroviruses or lentiviruses [11–13]. hiPSCs exhibit pluripotency, proliferation capability, and gene expression similar to those of human embryonic stem cells (hESCs), but do not present the same ethical problems. Immune rejection can be avoided by the establishment of hiPSC banks from donors with various human leukocyte antigen (HLA) types. Moreover, to reduce the risk of tumorigenicity, new methods for generating iPSCs without viral vectors have been developed [14–16]. Therefore, hiPSCs are viewed as a promising

Departments of [1]Medicine and Clinical Science and [2]Oral and Maxillofacial Surgery, Kyoto University Graduate School of Medicine, Kyoto, Japan.

new tool for regenerative medicine, disease pathogenesis studies, and drug screening. hESCs readily form cartilaginous tissues in teratomas in vivo, but the proportion of chondrocytes arising from spontaneous differentiation via embryoid body (EB) formation in vitro is very low. Three-dimensional (3D) pellet culture and micromass culture have been used successfully for in vitro chondrogenic differentiation of MSCs and mature chondrocytes [17–19]. These culture systems allow cell–cell interactions analogous to those that occur in precartilage condensation during embryonic development, and can induce terminal differentiation of mesenchymal progenitor cells into hypertrophic chondrocytes. Besides pellet culture and micromass culture, many attempts have been made to induce chondrocytes from ESCs in vitro, including coculture with irradiated articular chondrocytes [20] or limb bud progenitor cells from a developing embryo [21], culture with a conditioned medium [22], genetic manipulation (e.g., Sox9 expression) [23], and use of biomaterials [24]. However, both coculture with other animal cells and culture with a conditioned medium lack reproducibility and carry the risk of pathogen transmission. Genetic manipulation using virus-based vectors poses risks for clinical applications. Thus, in spite of the many efforts, an efficient culture method for inducing mature chondrocytes from hESCs has not yet been established.

hiPSCs have been reported to generate cartilaginous tissue in teratoma in vivo [11–13], but limited data exists at present regarding the in vitro chondrogenic differentiation of hiPSCs. When dissociated EB cells generated from fetal neural stem cell-derived hiPSCs were grown with a chondrogenic medium on agarose-coated wells, they expressed chondrogenic differentiation markers detectable by immunofluorescence staining [25]. However, immunofluorescence did not clearly reveal morphological characteristics of chondrocytes; a large and spherical shape with clear cytoplasm surrounded by an extracellular matrix [25]. Thus, a reproducible method for in vitro chondrogenic differentiation of hiPSCs must be established. Since hiPSC-derived chondrocytes can be used to study the pathogenesis of genetic disorders, such as skeletal dysplasia, and to develop drug screening systems for cartilage diseases, it would be desirable to develop in vitro differentiation methods that mimic physiological differentiation processes and do not require genetic manipulation.

In the current study, we examined the chondrogenic differentiation capability of hiPSCs by combining a pellet culture system, the most reliable method reported to date, with spontaneous differentiation via EB formation, which mimics early embryonic development by forming the 3 germ layers (mesoderm, ectoderm, and endoderm). We also compare and discuss the chondrogenic cells induced from hiPSCs and hESCs using our culture protocol.

Materials and Methods

Cell culture

hiPSC line 201B7 (B7) was previously generated by introducing 4 reprogramming factors (Oct3/4, Sox2, Klf4, and c-Myc) into dermal fibroblasts from the facial dermis of a 36-year-old Caucasian woman [11]. The hESC line H9 was obtained from the WiCell Research Institute (Madison, WI, www.wicell.org) [26]. These cells were maintained as previously described [11,27]. Briefly, murine embryonic fibroblasts (MEFs) were grown in the Dulbecco's modified Eagle's medium (DMEM; Invitrogen, Grand Island, NY, www.invitrogen.com), supplemented with 10% (vol/vol) fetal bovine serum (FBS; HyClone, Logan, UT, www.hyclone.com), 100 U/mL penicillin, and 100 μg/mL streptomycin (Invitrogen). MEF feeder layers were prepared by chemically inactivating subconfluent cultures with 10 μg/mL mitomycin C (Kyowa, Tokyo, Japan, www.kyowa.co.jp) for 3 h at 37°C and reseeding on 0.1% (wt/vol) gelatin-coated dishes. hiPSCs and hESCs were grown on inactivated MEF feeder layers in the primate ESC medium (ReproCELL, Kanagawa, Japan, www.reprocell.com) containing 4 ng/mL of basic fibroblast growth factor (bFGF) (ReproCELL).

Chondrogenic differentiation

For EB formation, hiPSC and hESC colonies were harvested by treating with 1 mg/mL collagenase type IV, and then plated onto suspension culture dishes, where they were allowed to aggregate in a maintenance medium without bFGF. After 7 days as a suspension culture, EBs were transferred to gelatin-coated dishes and cultivated for 1 week in DMEM containing 10% FBS, 100 U/mL penicillin, and 100 μg/mL streptomycin. EBs and cells sprouted from EBs were harvested and dissociated with 0.25% trypsin/EDTA (Life Technologies, Inc., Grand Island, NY, www.lifetechnologies.com). Dissociated cells were passed through a 100-μm cell strainer (BD Biosciences, Bedford, MA, www.bdbiosciences.com) to remove cell aggregates and cultivated in monolayers for another week in DMEM containing 10% FBS, 100 U/mL penicillin, and 100 μg/mL streptomycin. To induce chondrogenic differentiation, we used a previously described pellet culture system [18,28]. Cell suspensions containing 3×10^5 cells per 15-mL polypropylene tube were centrifuged to form a cell pellet. Cell pellets were cultivated at 37°C with 5% CO_2 for up to 21 days in the chondrogenic induction medium consisting of DMEM/F12 supplemented with 10% FBS, ITS+™ Premix (BD Biosciences), 50 μg/mL ascorbic acid 2-phosphate (Wako Pure Chemical Industries, Osaka, Japan, www.wako-chem.co.jp), 100 μg/mL sodium pyruvate, 100 nM dexamethasone, 10 ng/mL transforming growth factor-β3 (TGF-β3) (PeproTech Inc., Rocky Hill, NJ, www.peprotech.com), 100 U/mL penicillin, and 100 μg/mL streptomycin. The medium was replaced every 3 days. Pellet cultures were repeated and evaluated histologically 11 times using hiPSCs (B7) and 13 times using hESCs (H9).

Flow cytometry

Cells were incubated with saturating levels of antibodies for 1 h at 4°C. The following fluorescein isothiocyanate (FITC)- or phycoerythrin (PE)-conjugated antibodies recognizing human antigens were used: TRA-1-60 (No. 560380), CD44 (No. 348052), CD90 (No. 555596), CD106 (No. 555647), CD146 (No. 550315), CD166 (No. 559263), CD34 (No. 348057), and CD45 (No. 347463) (BD Biosciences); CD73 (No. 12-0739) and CD105 (No. 12-1057) (eBioscience, Inc., San Diego, CA, www.ebioscience.com); and CD140a (No. 323505) (BioLegend, San Diego, CA, www.biolegend.com). The anti-Stro-1 monoclonal antibody (MAB1038) was purchased from

R&D Systems, Inc. (Minneapolis, MN). Each analysis included corresponding FITC- or PE-conjugated isotype controls. Samples were run on a Becton Dickinson FACScan flow cytometric system (BD Biosciences), and analysis was completed using FlowJo Software (FlowJo, Ashland, OR, www.flowjo.com).

Real-time reverse transcription–polymerase chain reaction

Total RNA was extracted from cell pellets using the RNeasy® Mini Kit (Qiagen, Chatsworth, CA, www.qiagen.com). To ensure the complete removal of DNA, we included a 15-min DNase I (Qiagen) treatment before the washing step. First-strand cDNA synthesis was performed using TaqMan® Reverse Transcription Reagents (Applied BioSystems, Carlsbad, CA, www.appliedbiosystems.com) with random hexamers. Real-time reverse transcription–polymerase chain reaction (RT-PCR) was performed in a StepOne™ real-time PCR System (Applied BioSystems). Complementary DNA was mixed with TaqMan Universal PCR Master Mix (Applied BioSystems) and TaqMan Gene Expression Assay (Applied BioSystems) primers: Sox9 (*SOX9*, Assay ID; Hs00165814_m1), type II collagen (*COL2A1*, Hs01060345_m1), aggrecan (*ACAN*, Hs00153936_m1), type X collagen (*COL10A1*, Hs00166657_m1), and GAPDH (*GAPDH*, Hs99999905_m1). All RNA samples were titrated to yield equal amplification of GAPDH as an internal normalization control. Reactions for each sample were performed in triplicate. After an initial denaturation step (95°C for 10 min), amplification was performed for 45 cycles (15-s denaturation at 95°C and 60-s extension at 60°C).

Histological analysis

Cell pellets were fixed in 2% paraformaldehyde, dehydrated, and embedded in paraffin. The sections were cut at a thickness of 4 μm and stained with Alcian blue and toluidine blue, as previously described [28]. For immunohistochemical analysis, a labeled streptavidin–biotin staining kit (LSAB2 System-HRP) (Dako, San Antonio, TX, www.dako.com) was used. The sections were incubated overnight at 4°C with the following primary antibodies: anti-type II collagen (F-57; Daiichi Fine Chemical, Takaoka, Toyama, www.daiichi-fcj.co.jp), anti-aggrecan (sc-70333; Santa Cruz Biotechnology, Inc., Santa Cruz, CA, www.scbt.com), and anti-mitochondria (MAB1273; Millipore, Billerica, MA, www.millipore.com). Normal human articular chondrocytes from knee cells (NHAC-kn) (Lonza Walkersville, Inc., Walkersville, MD, www.lonza.com) were grown using the same pellet culture protocol as that used for hiPSCs and hESCs, and were used as a positive control. Cell pellets derived from human BMMSCs (Lonza Walkersville, Inc.) were cultivated in DMEM/F12 supplemented with 10% FBS, 100 U/mL penicillin, and 100 μg/mL streptomycin, and were used as a negative control.

Statistical analysis

Real-time RT-PCR experiments were performed independently at least 3 times and gave highly similar results. Data are presented as the mean ± SD. Statistical analysis was performed using one-factor analysis of variance. Differences were considered statistically significant when $P < 0.05$.

Results

Mesenchymal differentiation of hiPSCs via EB formation

We used a multistep culture method combining spontaneous differentiation via EB formation, cell outgrowth from EBs on gelatin-coated dishes, monolayer culture after cell dissociation into single cells, and 3D pellet culture (Fig. 1). Chondrogenic progenitor cells are derived from MSCs, which originate from the mesoderm and neural crest. Therefore, we first tried to promote differentiation of undifferentiated hiPSCs into the mesenchymal lineage. hiPSCs contained in EBs retained pluripotency in vitro; we used immunofluorescence analysis to confirm the expression of markers for mesoderm (α-smooth muscle actin), ectoderm (β3-tubulin), and endoderm (forkhead box A2; FOXA2) on cultured EBs (Supplementary Fig. S1; Supplementary Data

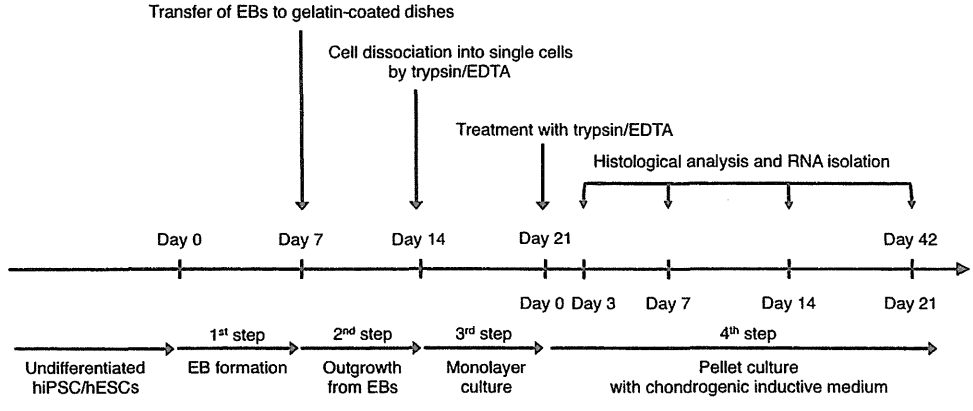

FIG. 1. Schematic diagram of the culture protocol for chondrogenic differentiation of human induced pluripotent stem cells (hiPSCs) and human embryonic stem cells (hESCs). The differentiation culture protocol consists of 4 steps: (1) Embryoid body (EB) formation in suspension culture dishes; (2) Cell outgrowth from EBs on gelatin-coated dishes; (3) Monolayer culture under mesenchymal stem cell (MSC) growth conditions after dissociation into single cells by trypsin/EDTA; and (4) Three-dimensional pellet culture in the chondrogenic induction medium. During pellet culture, histological and gene expression analyses were performed at days 3, 7, 14, and 21.

are available online at www.liebertpub.com/scd). Before proceeding to pellet culture, we included a monolayer culture step to exclude residual undifferentiated cells present in the EBs as well as to expand cells committed to the mesenchymal lineage. These cells were able to attach to regular culture dishes and proliferate in the MSC growth medium consisting of DMEM supplemented with 10% FBS. In our experience, the initial cell density was critical for monolayer culture. To determine the ideal cell density, we used trypsin/EDTA to dissociate cells that had sprouted from EBs and seeded them at serial dilutions ranging from 0.05 to 20×10^4 cells/cm^2. We found that a cell density of $1–2\times10^4$ cells/cm^2 was ideal for cell proliferation in monolayer culture (Fig. 2). Seeding at a low cell density induced mitotic arrest and a large, flattened, and irregular cell morphology. Inversely, when seeded at a high cell density, cells formed clusters and proliferated in 3 dimensions. The cell proliferation rate in monolayers decreased, but did not drop to zero, after 7 days of culture (Supplementary Fig. S2). The culture period in the monolayer had no apparent effect on the differentiation capability (Supplementary Fig. S3). Therefore, we seeded cells at $1–2\times10^4$ cells/cm^2 and cultivated the resulting monolayers for 7 days in the remaining experiments.

Next, before proceeding to pellet culture, we analyzed the expression of cell surface markers on hiPSCs in monolayer culture. Flow cytometric analysis demonstrated that the majority of hiPSCs expressed CD90 (Thy-1), CD44, and CD166 (activated leukocyte cell adhesion molecule) (Fig. 3). A small fraction of hiPSCs was positive for CD146 (MUC18), CD73, CD105 (endoglin), and CD140a (platelet-derived growth factor receptor α [PDGFRα]) (Fig. 3). CD73, CD90, CD105, CD44, CD166, and CD146 are known to be markers for MSCs [29,30]. PDGFRα is a marker for paraxial mesodermal cells, from which cartilage tissues originate, especially in mouse development [31]. TRA-1-60, an undifferentiated cell marker both for hiPSCs and hESCs, was not detected in monolayer-cultured hiPSCs (Fig. 3), suggesting that the multistep culture process promoted differentiation of hiPSCs. CD34 and CD45, hematopoietic markers that are not expressed in MSCs [29], were also not detected in monolayer-cultured hiPSCs (Fig. 3). However, we did not detect the expression of the MSC markers Stro-1 and CD106. Stro-1 has been established as a monoclonal IgM derived from mice immunized with human CD34-positive bone marrow cells [32]. Recently, it was reported that Stro-1 is a 75-kDa endothelial antigen, and that its expression on MSCs might result from induction of MSCs to endothelial lineage [33]. Monolayer-cultured hiPSCs in our method may commit to differentiating into mesenchymal lineage cells, which do not contain endothelial antigens. Furthermore, few reports have demonstrated the expression of Stro-1 on MSCs derived from hiPSCs and hESCs, although many attempts have been made to induce MSCs from hiPSCs and hESCs [34]. In a recent report describing one-step derivation of MSC-like cells from hiPSCs, MSC-like cells did not express Stro-1, although the cells clearly expressed CD73, CD90, CD105, CD144, and CD166 [35]. A Nestin(+)/CD271(−)/Stro-1(−) cell population from hESCs was recently reported to be mesenchymal-like precursors [36]. MSCs induced from hiPSCs or hESCs in vitro may exhibit different characteristics, including surface marker expression, from those of MSCs isolated primarily from bone marrow and other organs. CD106 is also known as vascular cell adhesion molecule-1 [37]. Several groups have reported changes in the expression of cell surface markers, including CD106, following prolonged cultivation [37,38]. Treatment with hyaluronan, a major glycosaminoglycan ligand of CD44, has also been reported to upregulate the expression of CD106 in MSCs [39]. Thus, it is possible that our culture method, which consists of 3 weeks of culture under 3 different conditions, attenuates the expression of

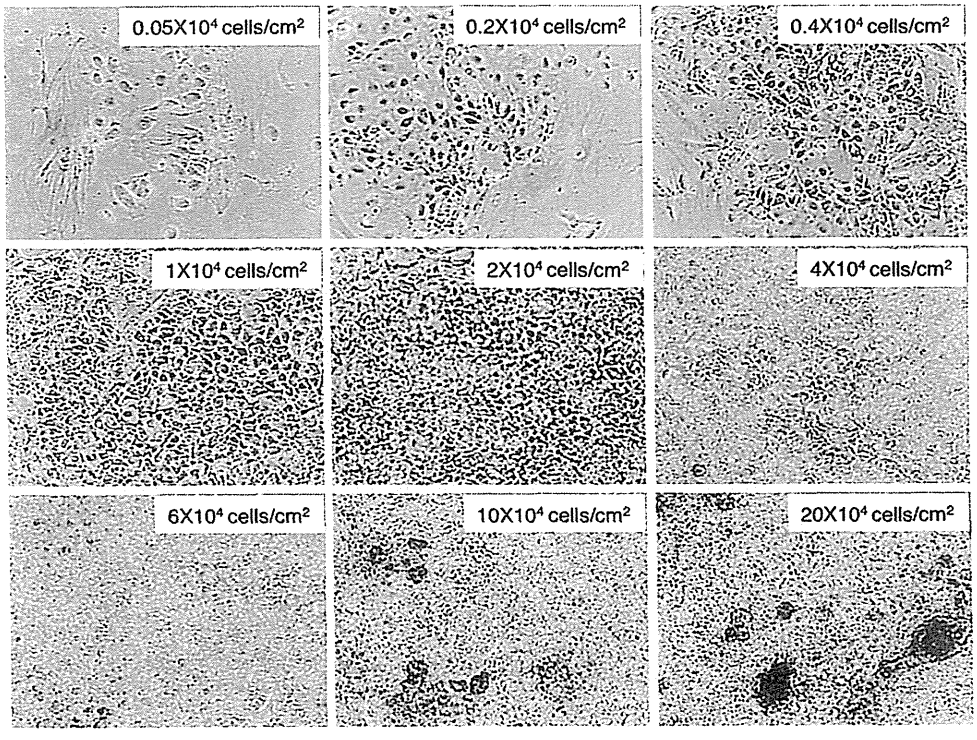

FIG. 2. Ideal cell density of hiPSCs for monolayer culture. Phase-contrast micrograph of monolayer cultured hiPSCs at 40× magnification 7 days after plating onto adhesive culture dishes. To determine the ideal cell density, sprouted cells from EBs were dissociated by trypsin/EDTA and serially diluted to yield cell densities of $0.05–20\times10^4$ cells/cm^2. A cell density at $1–2\times10^4$ cells/cm^2 was determined to be ideal for cell proliferation without cell aggregation.

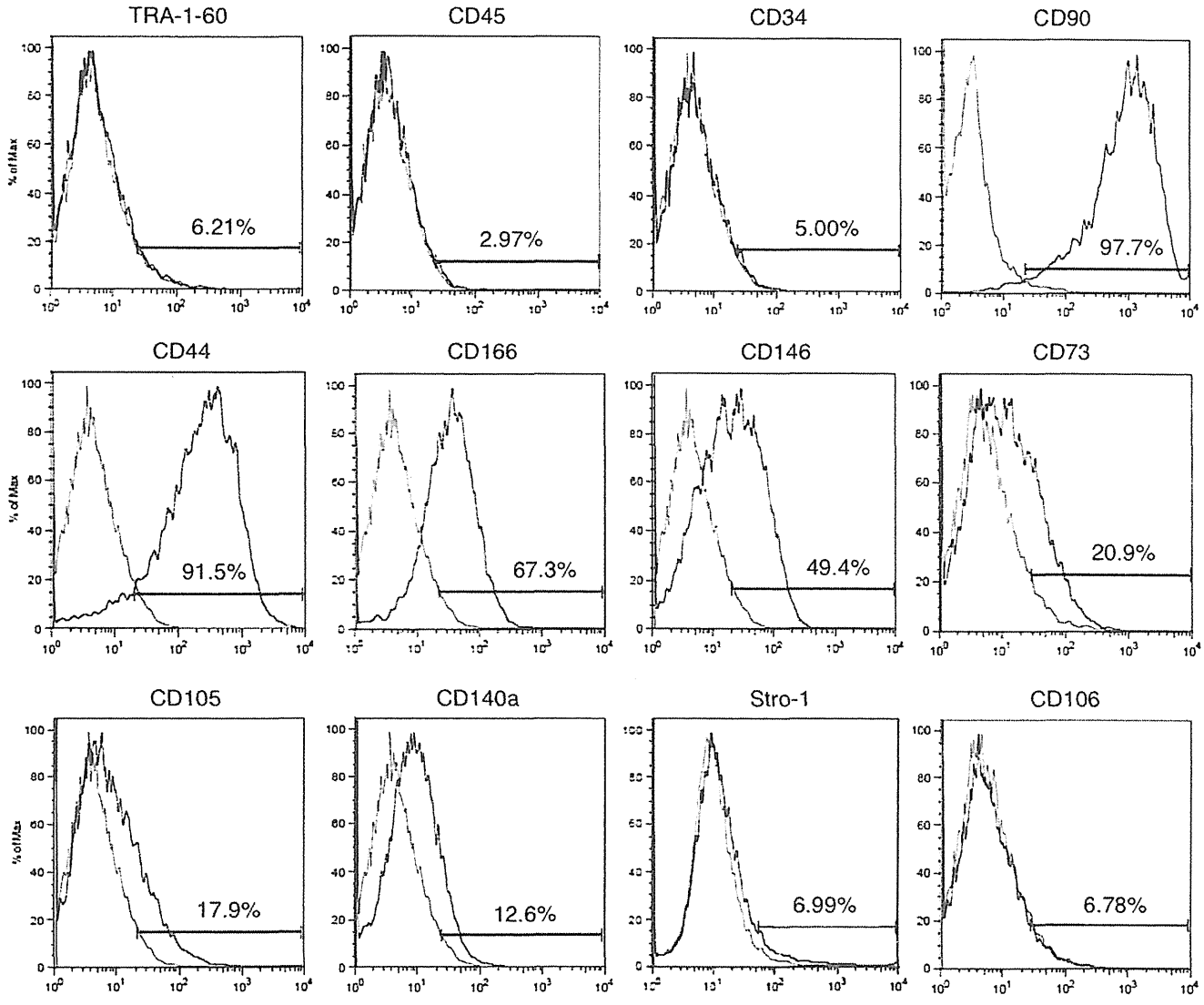

FIG. 3. Expression of MSC markers by monolayer cultured hiPSCs. Cells were cultivated in monolayer culture under MSC growth conditions for 7 days, and then dissociated by trypsin/EDTA for pellet culture. Flow cytometric analysis of cell surface marker expression on dissociated hiPSCs revealed that the major fraction of hiPSCs expressed CD90, CD44, and CD166, and that a fraction of hiPSCs expressed CD146, CD73, CD105, and CD140a. hiPSCs were negative for TRA-1-60, a marker of undifferentiated cells, and for hematopoietic markers (CD34 and CD45). Gray lines show staining with the relevant isotype-matched control antibodies.

CD106. Nonetheless, expression of CD90, CD44, CD166, CD146, CD73, CD105, and CD140a and the lack of CD34 and CD45 suggest that at least a fraction of hiPSCs in monolayer culture differentiated along the mesenchymal lineage. Indeed, osteogenic differentiation of monolayer-cultured hiPSCs was confirmed using a previously described induction medium [7] (data not shown).

Chondrogenic differentiation of hiPSCs by pellet culture

The original in vitro chondrogenic differentiation method was initially established using rabbit and human bone marrow-derived mesenchymal progenitor cells [17,18]. The high-density 3D microenvironment is thought to facilitate cell–cell and cell–matrix interactions and to mimic in vivo limb development, in which mesenchymal condensation occurs before chondrogenic induction. In a pellet or micromass culture system, cells change their morphology, express chondrogenic differentiation markers, and produce an extracellular matrix that contains acidic proteoglycans, which stain positive for Alcian blue and toluidine blue. In a previous report, micromass culture using hESCs dissociated from EBs exhibited chondrogenesis superior to that of a two-dimensional (2D) EB direct-plating outgrowth system [40].

In the present study, we dissociated EBs and selected only the cells that proliferated in monolayer culture in the MSC growth medium. After 3 days of pellet culture, little Alcian blue staining was observed, and hiPSCs inside the pellet exhibited fibroblast-like morphology (Fig. 4A). At day 7 of induction, pellets showed partial Alcian blue staining and contained some large spherical cells with typical chondrocyte-like morphology (Fig. 4A). At day 14 of induction, spherical cells and interstitium, which was clearly stained

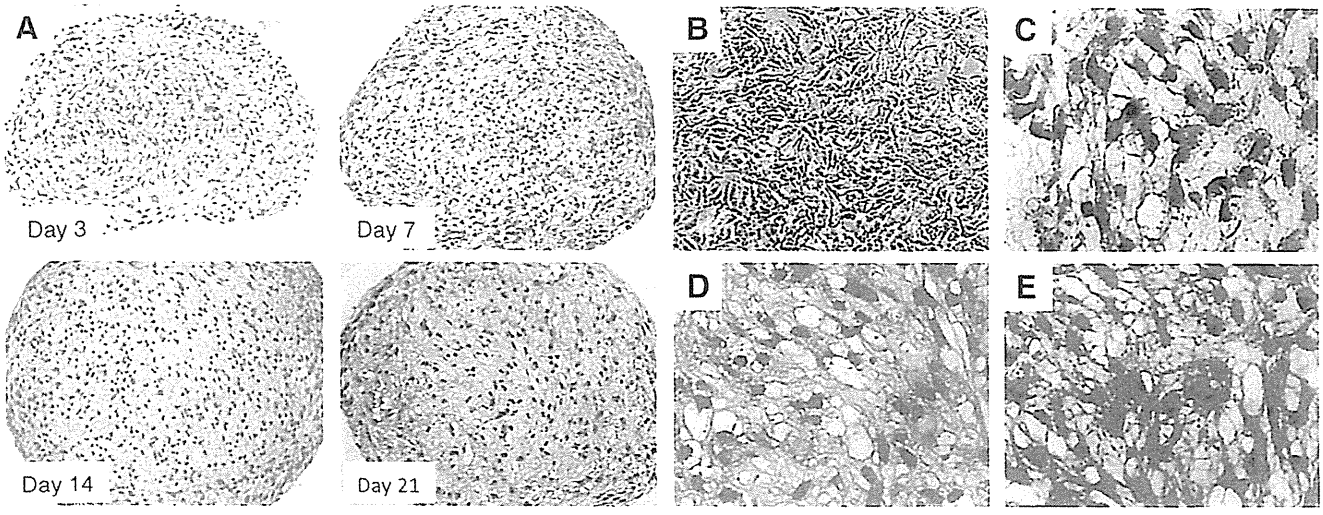

FIG. 4. Histological analysis of chondrogenic differentiation from hiPSCs (B7). Histological analysis of paraffin-embedded cell pellets stained with Alcian blue/hematoxylin/eosin (HE) revealed progressive chondrogenic differentiation of hiPSCs. The positive area and intensity of Alcian blue staining, which indicated the existence of acidic proteoglycans, increased progressively **(A)**. hiPSCs in monolayer culture before pellet culture exhibited small size and fibroblast-like morphology **(B)**. After pellet culture for 21 days, staining with HE revealed spherical cell morphology and interstitium **(C)**. Micrographs at high magnification revealed positive staining with Alcian blue **(D)** and metachromasy of toluidine blue **(E)** in interstitium of pellets cultured in the chondrogenic induction medium for 21 days. **(A)**, 100× magnification; **(B)**, 40× magnification; **(C–E)**, 200× magnification.

with Alcian blue, were evident throughout the pellet (Fig. 4A). At day 21 of induction, the entire pellet was intensely stained with Alcian blue, suggesting maturation of cartilaginous extracellular matrix (Fig. 4A).

Before chondrogenic induction by pellet culture, hiPSCs in monolayer culture were small and fibroblast-like (Fig. 4B). However, at day 21 of induction, hiPSCs located inside the pellet exhibited large spherical morphology (Fig. 4C) and were surrounded by Alcian blue–positive (Fig. 4D) and toluidine blue–positive (Fig. 4E) acidic proteoglycans. At day 28 of induction, many pellets exhibited internal necrosis (data not shown). Thus, in our method, the differentiation of hiPSCs appeared to reach a plateau at day 21 of induction. The cell morphology and positive staining for Alcian blue and toluidine blue indicated that hiPSCs differentiated into the chondrogenic lineage. To confirm the chondrogenic differentiation capability of hiPSCs, we examined 2 more hiPSC lines. One line (iPS-TIG107) was generated from TIG-107

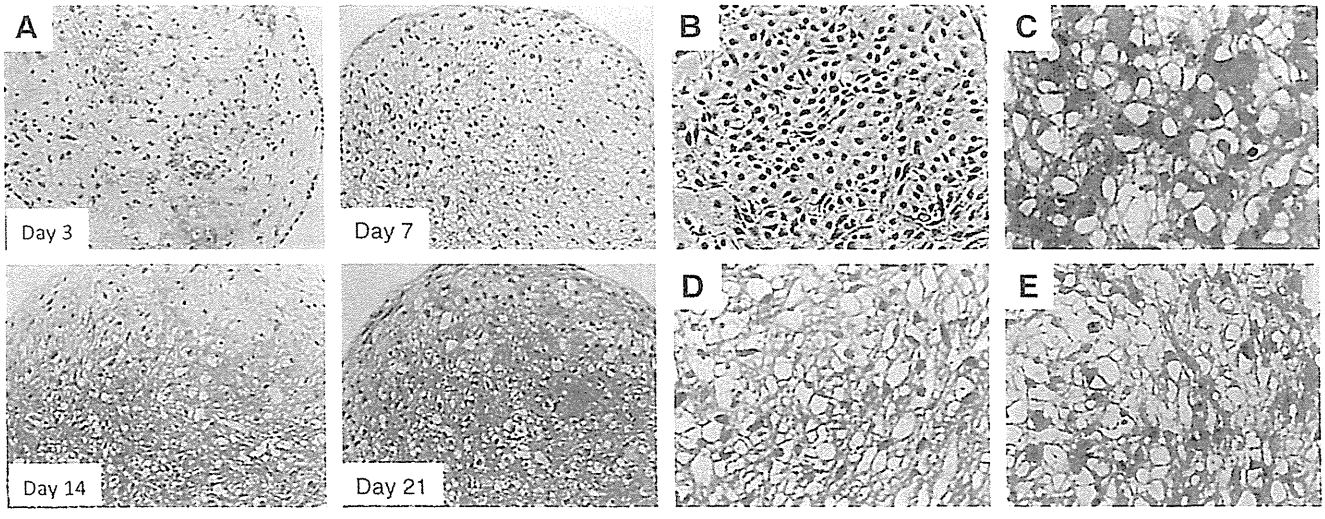

FIG. 5. Histological analysis of chondrogenic differentiation from hESCs (H9). Histological analysis of hESC-derived pellets stained with Alcian blue/HE indicated progressive chondrogenic differentiation similar to that observed with hiPSCs. The positive area and intensity of Alcian blue staining increased progressively **(A)**. hESCs in monolayer culture before pellet culture exhibited morphology similar to that of hiPSCs in monolayer culture **(B)**. After pellet culture for 21 days, staining with HE revealed spherical morphology typical of chondrocytes and interstitium **(C)**. hESCs also presented positive staining with Alcian blue **(D)** and metachromasy of toluidine blue **(E)** in interstitium of pellets cultured with chondrogenic induction medium for 21 days. **(A)**, 100× magnification; **(B)**, 40× magnification; **(C–E)**, 200× magnification.

fibroblasts derived from the skin of an 81-year-old Japanese woman by introducing 4 reprogramming factors using retroviruses. Another line, 253G1 (G1), was derived from the same donor as B7, but generated by introducing 3 factors (Oct 3/4, Sox2, and Klf4, but not c-Myc) using retroviruses [41]. These 2 iPSC lines (iPS-TIG107 and G1) exhibited chondrogenic differentiation capability and time course similar to those of B7 (Supplementary Fig. S4 and S5), although the level of matrix synthesis appeared to be smaller in G1-derived pellets.

Comparative analysis of chondrogenic differentiation capability of hiPSCs and hESCs

We performed the procedure described above with hESCs (H9) and compared their chondrogenic differentiation capability to that of hiPSCs. During 21 days of induction, hESCs demonstrated a sequence of histological changes similar to that observed with hiPSCs (Fig. 5A). At day 3 of induction, some areas of hESC-derived pellets were faintly stained with Alcian blue, and some hESCs already exhibited chondrocyte-like spherical morphology. At day 7 of induction, the whole hESC-derived pellet was stained with Alcian blue. In comparison, hiPSC-derived pellets showed only partial staining at this time. At day 14 of induction, the whole pellet was more strongly stained with Alcian blue. At day 21 of induction, the appearance of cells with chondrocyte-like morphology and Alcian blue staining of the interstitium were more apparent, although the difference between days 14 and 21 was not significant. Thus, compared to hiPSCs, hESCs exhibited slightly faster progression of chondrogenic induction. Before chondrogenic induction by pellet culture, the morphology of monolayer-cultured hESCs was also fibroblast-like, similar to that of hiPSCs (Fig. 5B).

hESCs began showing morphological changes at day 3, and matured progressively thereafter (Fig. 5C). At day 21, the hESC-derived pellets showed intense Alcian blue staining (Fig. 5D) and toluidine blue metachromasy (Fig. 5E), as was the case for hiPSCs. At day 28 of induction, many hESC-derived pellets also exhibited internal necrosis (data not shown). About 85% of hESC-derived pellets (11 successful pellets/13 experiments), compared to 73% of hiPSC-derived pellets (8 successful pellets/11 experiments), exhibited successful chondrogenic differentiation. We also applied this culture protocol to another hESC line, KhES-1 [42], and found that it exhibited similar chondrogenic differentiation (Supplementary Fig. S6). These data demonstrate that in our multistep culture method, both hiPSCs and hESCs differentiate into the chondrogenic lineage, although hESCs exhibited slightly faster progression and increased efficiency of chondrogenic differentiation compared to hiPSCs.

Time course of gene expression of chondrogenic differentiation markers

We analyzed the time course of chondrogenic differentiation marker expression by real-time RT-PCR. The chondrogenic transcription factor Sox9 is required for precartilage condensation and directly regulates the transcription of type II collagen and aggrecan [43–45]. Type II collagen is an early chondrogenic differentiation marker, and aggrecan is a major sulfated proteoglycan of the cartilage matrix and a highly specific marker of differentiated chondrocytes [45]. *SOX9* expression was already present in hiPSCs at day 0 of monolayer culture (Fig. 6A), temporarily decreased at day 3 before the elevation of expression of *COL2A1* and *ACAN*, and gradually increased thereafter. *COL2A1* exhibited low expression at day 0, but was gradually upregulated at day 3 and 7, and was over 60-fold upregulated by day 14 (Fig. 6B). The expression of *ACAN* was also quite low initially (at days 0 and 3), but was dramatically upregulated at day 7 and increased further thereafter (Fig. 6C). The expression of *COL10A1*, a specific marker for hypertrophic chondrocytes,

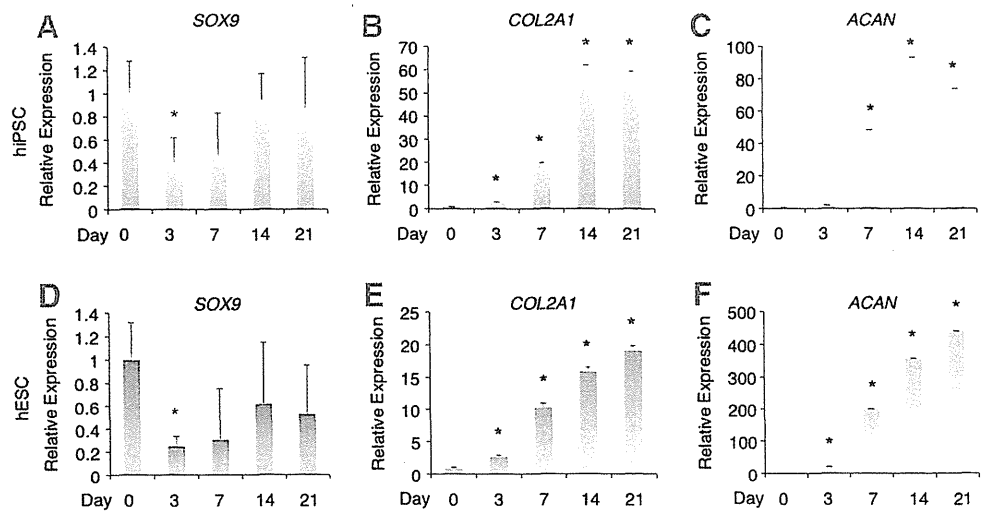

FIG. 6. Marker gene expression during chondrogenic differentiation of hiPSCs and hESCs. The expression of chondrogenic differentiation markers was analyzed by real-time reverse transcription–polymerase chain reaction. Both hiPSCs and hESCs in monolayer culture exhibited high expression of *SOX9* **(A** and **D)**. After the expression of *SOX9* was downregulated, the expression of type II collagen (*COL2A1*) **(B** and **E)** and aggrecan (*ACAN*) **(C** and **F)** increased progressively, especially from day 7 onward. The expression of *SOX9* was increased again at later stages (day 14 and 21). No type X collagen (*COL10A1*) expression was detected in either hiPSCs or hESCs (data not shown). *Significant change relative to control (day 0) ($n=3$). Data are shown as the mean ± SD.

was not detected at any time during the culture period (data not shown). hESCs showed similar trends in *SOX9*, *COL2A1*, and *ACAN* expression, but the increase in *COL2A1* levels was more modest, and the increase of *ACAN* was larger in hESCs than in hiPSCs (Fig. 6D–F). *COL10A1* expression was not detected in hESCs at any time during the culture period (data not shown).

Immunohistochemical analysis of chondrogenic differentiation markers

After confirming the expression of chondrogenic differentiation markers in both hiPSC- and hESC-derived culture pellets at the mRNA level, we next examined the expression of these markers by immunohistochemistry. Sections of hiPSC-derived pellets stained with hematoxylin/eosin (HE) exhibited spherical cell morphology characteristic of chondrocytes (Fig. 7A). Although we tried several different antibodies, we detected no type II collagen signal in hiPSC-derived pellets at day 21 of induction (Fig. 7B). Weak aggrecan expression was detected in hiPSC-derived pellets at day 21 of induction (Fig. 7C). Staining of NHAC-kn-derived pellets with HE revealed large spherical cell morphology and rich interstitium, suggesting greater maturation in NHAC-kn-derived pellets than in hiPSC-derived pellets (Fig. 7E). Unlike hiPSC-derived pellets, NHAC-kn-derived pellets exhibited strong positive staining both for type II collagen and aggrecan (Fig. 7F, G). Human BMMSC (hBMMSC)-derived pellets were cultivated in DMEM/F12, which contained only 10% FBS, 100 U/ml penicillin, and 100 μg/ml streptomycin, for 21 days as negative control. hBMMSC-derived pellets did not exhibit cell morphological change (Supplementary Fig. S7A) or the expression of chondrogenic markers; Type II collagen (Supplementary Fig. S7B) and aggrecan (Supplementary Fig. S7C). Positive signals for human-specific mitochondria in the hiPSC-, NHAC-kn-, and hBMMSC-derived specimens (Fig. 7D, H, Supplementary Fig. S7D) suggested that lack of staining for chondrogenic markers was not due to a general loss of antigenicity during specimen processing. In the specimens from hESC-derived pellets, type II collagen was not detected, and aggrecan was weakly detected, as with the hiPSC-derived pellets (data not shown). Taken together, these data suggested that hiPSCs and hESCs differentiated into chondrogenic lineage cells with similar characteristics, but neither hiPSCs nor hESCs yielded fully mature chondrocytes.

Discussion

In this study, we developed a simplified, reproducible method for differentiating hiPSCs into the chondrogenic lineage in vitro. Our method does not involve genetic manipulation, making it suitable for studying the mechanism of idiopathic genetic diseases, such as skeletal dysplasia, and for evaluating drug effects on chondrocytes. Our protocol consists of 4 steps: (1) EB formation, which involves spontaneous differentiation and mimics the formation of the 3 germ layers in vitro; (2) Cell outgrowth from EBs to increase cell number; (3) Monolayer culture to remove undifferentiated cells and select cells that can adapt to MSC growth conditions; and (4) 3D pellet culture, which is important for cell–cell and cell–matrix interactions. Our pellet culture medium was supplemented with TGF-β3 and dexamethasone, since these factors were previously demonstrated to produce the highest chondrogenic potential in 3D culture reported to date [46]. In our protocol, differentiation into the mesenchymal lineage during EB formation and monolayer culture was critical. In addition, cell density was a crucial factor for monolayer

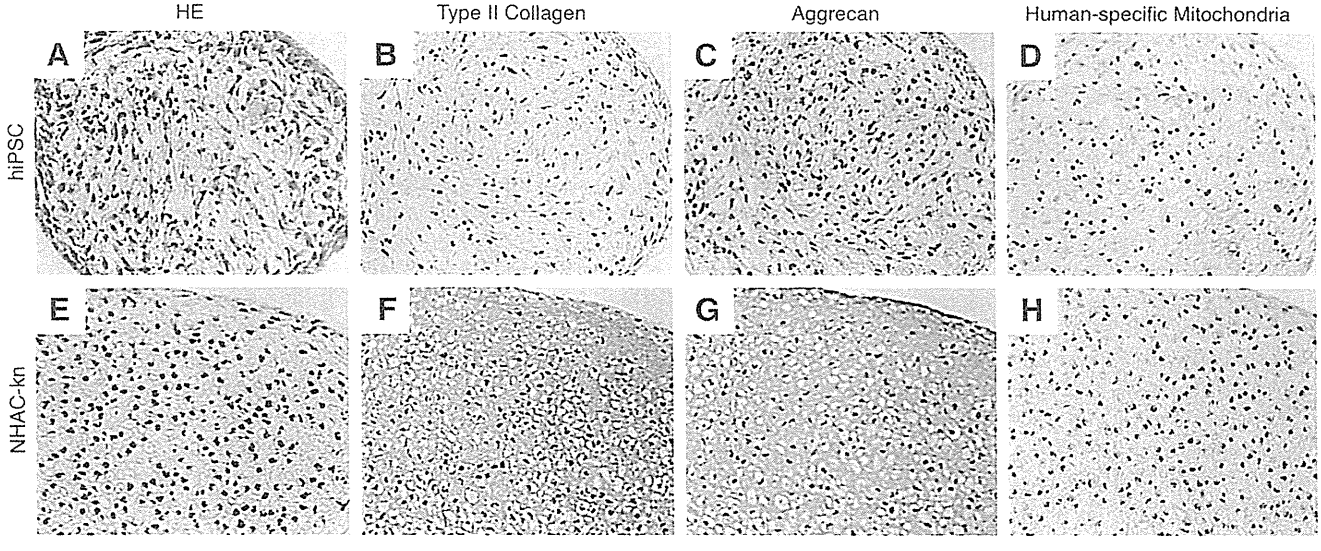

FIG. 7. Immunohistochemical analysis of chondrogenic differentiation markers in pellets derived from hiPSCs. Sections from paraffin-embedded hiPSC pellets cultivated for 21 days in the chondrogenic induction medium were stained with HE **(A)**. Normal human articular chondrocytes from knee cells (NHAC-kn) cultivated for 21 days according to the same pellet culture protocol, used as a positive control, were also stained with HE **(E)**. Sections in both **(A)** and **(E)** contained large spherical cells typical of chondrocytes and rich interstitium that was positive for Alcian blue (data not shown). Immunohistochemical staining of hiPSC-derived pellets failed to detect expression of type II collagen **(B)**. Staining for aggrecan was faintly positive **(C)**. The sections from NHAC-kn stained strongly for both type II collagen **(F)** and aggrecan **(G)**. Human-specific mitochondrial staining was detected in both the hiPSC-derived pellet **(D)** and NHAC-kn–derived pellet **(H)**. **(A–H)**, 100× magnification.

culture in our method was the same as that previously reported for induction of chondrocytes from hESCs in an arginine-glycine-aspartate–modified hydrogel combined with EB formation and monolayer culture [47], suggesting that the optimal culture condition for chondrogenic differentiation of hiPSCs is very close to that of hESCs.

Other attempts to induce MSCs from ESCs and iPSCs have also been reported. For instance, MSCs or MSC-like cells have been derived from hESCs by either transfection of a human telomerase reverse transcriptase (hTERT) gene [48] or by coculture with mouse OP9 cells [34]. However, the use of exogenous genetic material or mouse cells in those protocols introduces, respectively, the risk of tumorigenicity or contamination by animal pathogens. To overcome these problems, hESCs have been plated directly on gelatin-coated dishes without EB formation and cultured with bFGF and PDGF-AB [49]. In that study, after 1 week, CD105-positive and CD24-negative cells were sorted as MSCs. Those cells expressed MSC markers, such as CD44, CD49a, CD105, and CD166. However, expression of type II collagen mRNA decreased progressively after chondrogenic induction, even though the immunostaining for type II collagen was positive. Recently, mesenchymal progenitor cells were induced from murine iPSCs using a method similar to ours [50]. In that method, murine iPSC-derived EBs were transferred to culture dishes and cultivated in DMEM supplemented with 10% FBS and 10^{-6} M *all-trans* retinoic acid. Sprouted cells from EBs were dissociated with trypsin/EDTA, seeded onto gelatin-coated dishes, and cultivated in the MesenPRO RS™ Medium (Invitrogen) supplemented with bFGF. The resulting induced mesenchymal progenitor cells expressed markers for MSCs. Thus, a culture protocol consisting of EB formation, cell outgrowth from EBs, and monolayer culture after dissociation into single cells appears to be suitable for mesenchymal differentiation from iPSCs and ESCs. This method is simple, reproducible, and results in good cell viability, although some details still need to be refined. In the present study, to reduce the risk of cell damage, we did not use cell sorting. However, purification of mesenchymal progenitor cells by cell sorting may improve the efficiency of chondrogenic differentiation, and should be combined with our approach in future studies.

The expression of sequential markers of chondrogenic differentiation in vitro is inconsistent among studies. Sox9 belongs to the Sry-related high-mobility-group box (Sox) transcription factors and directly regulates the expression of several chondrogenic markers, including type II collagen and aggrecan [43–45]. Sox9 was identified as a causative gene of campomelic dysplasia, with heterozygous patients exhibiting disproportionately short stature, bowing of the limbs, low ears, depressed nasal bridge, talipes equinovarus, long philtrum, and micrognathis [51,52]. Heterozygous Sox9 mouse mutants exhibited the same skeletal abnormalities as campomelic dysplasia patients, and histological analysis revealed smaller and delayed chondrogenic mesenchymal condensation and enlargement of the hypertrophic zone in association with premature mineralization [53]. During mouse embryogenesis, Sox9 is expressed in all chondroprogenitors and chondrocytes except for hypertrophic chondrocytes. Thus, Sox9 is required for the commitment of undifferentiated MSC to the chondrogenic lineage, for mesenchymal condensation, and for inhibiting hypertrophic conversion of proliferating chondrocytes. Gong *et al.* reported that micromass culture using hESCs (H9) resulted in chondrogenic differentiation, with Sox9 expression elevated at the early stage and strikingly downregulated at the intermediate stage of inductive culture [54]. In their report, no type X collagen expression was detected even at late stages of induction, which the authors deemed favorable, because chondrocytes in articular cartilage do not normally undergo hypertrophic maturation. Meanwhile, a report by Toh *et al.*, in which hESCs (line H1 and H9) were differentiated into hypertrophic chondrocytes following micromass culture of EB-derived cells, demonstrated the expression of type X collagen, which was detected by both PCR and immunohistochemistry [40]. However, in another report Toh *et al.* induced chondrogenic differentiation of hESCs (H9) by a combination of micromass culture of EB-derived cells and pellet culture after cell dissociation; they demonstrated that Sox9 expression increased continuously for 21 days in micromass culture, whereas no type X collagen expression was detected even after pellet culture for another 4 weeks [55]. In a recent study, chondrocytes could be induced from hESCs in 2D culture by a multistep process that applied different cell density and different combinations of growth factors to each stage [56]. In that study, differentiated cells expressed Sox9, CD44, and type II collagen, but did not express type X collagen. In our experiments, the expression of *SOX9* was already elevated at the start of pellet culture, decreased promptly, and increased again at a later stage. Because Sox9 inhibits hypertrophic conversion of proliferating chondrocytes [53], increased expression of *SOX9* at a late stage might explain why the expression of type X collagen was not detected at any time during the culture period. Moreover, negative expression of type X collagen is not necessarily unfavorable, because hyaline cartilage, which constitutes articular cartilage, does not express type X collagen [54].

The cause of the discrepancy between gene expression and protein expression in cell pellets needs to be elucidated. Although RT-PCR revealed that expression of type II collagen and aggrecan mRNAs was obviously increased, immunohistochemistry detected only weak staining for aggrecan and no staining for type II collagen. The reason for negative immunostaining of type II collagen is not known. However, a discrepancy between gene expression and protein expression of type II collagen has been reported previously, suggesting that mRNAs containing AU-rich elements are destabilized when translated [49]. There is a possibility that translation might be destabilized in our culture conditions. Another possibility is that cells in pellets are still immature chondrocytes, and do not produce enough collagen to be detected by immunohistochemistry. To achieve in vitro chondrogenic differentiation, 3D pellet culture in the presence of TGF-β superfamily members seems to be essential. While pellet culture is definitely an effective tool, it is not without its limitations. Another critical factor is oxygen tension. The physiological environments of both articular cartilage and bone marrow exist within a range of 1%–7% oxygen. Previous studies have shown that hypoxia promotes chondrogenic differentiation of MSCs [57,58] and that hypoxia increases the expansion potential of MSCs [59,60]. Additionally, Sox9 is upregulated by hypoxia, resulting in increased expression of type II collagen and aggrecan in human articular chondrocytes. Thus, it is possible that

hypoxic culture conditions would promote chondrogenic differentiation of hiPSCs in combination with our protocol. In addition, the combination of TGF-β in the induction medium with various growth factors, such as growth and differentiation factor 5 [61], cell sorting by MSC markers, and subjecting cultures to cyclic hydrostatic pressure [62] might also improve maturation of chondrocytes in our method, resulting in enhanced expression of type II collagen and aggrecan protein.

In our method, the ability of hESCs to differentiate into the chondrogenic lineage was similar to that of hiPSCs, although hESCs exhibited slightly faster progression and greater efficiency of chondrogenic differentiation compared to hiPSCs. However, a slight difference in the progression and efficiency of chondrogenic differentiation might arise from clonal variation, since different ESC and iPSC lines can vary in their characteristics [63,64]. In our study, G1-derived pellets seemed to produce less matrix than B7 and iPS-TIG107 lines. It is difficult for our method to control evenly the differentiation time course and the characteristics of induced chondrocytes from different cell lines.

In conclusion, we have developed a simplified and reproducible culture method that allows hiPSCs and hESCs to be differentiated into the chondrogenic lineage via generation of mesenchymal progenitor cells. Although the inductive culture method still needs improvement, our study provides an important foundation for cartilaginous tissue engineering, which will benefit regenerative medicine, pathogenesis studies of idiopathic skeletal dysplasia, and the development of drug screening systems for cartilaginous diseases.

Acknowledgments

We thank J. Toguchida and A. Nasu, Center for iPS Cell Research and Application, Kyoto University, and H. Yao, Department of Transfusion Medicine and Cell Therapy, Kyoto University, for technical advice. This work was supported by the project for realization of regenerative medicine and Grant-in-Aid for Scientific Research (22591009) from the Ministry of Education, Culture, Sports, Science and Technology of Japan, Grant-in-Aid for Scientific Research from the Ministry of Health, Labor, and Welfare of Japan, and Novo Nordisk Study Award for Growth and Development 2011.

Author Disclosure Statement

The authors indicate no potential conflict of interests.

References

1. Nejadnik H, JH Hui, EP Feng Choong, BC Tai and EH Lee. (2010). Autologous bone marrow-derived mesenchymal stem cells versus autologous chondrocyte implantation: an observational cohort study. Am J Sports Med 38:1110–1116.
2. Wakitani S, T Okabe, S Horibe, T Mitsuoka, M Saito, T Koyama, M Nawata, K Tensho, H Kato, et al. (2011). Safety of autologous bone marrow-derived mesenchymal stem cell transplantation for cartilage repair in 41 patients with 45 joints followed for up to 11 years and 5 months. J Tissue Eng Regen Med 5:146–150.
3. Wakitani S, M Nawata, K Tensho, T Okabe, H Machida and H Ohgushi. (2007). Repair of articular cartilage defects in the patello-femoral joint with autologous bone marrow mesenchymal cell transplantation: three case reports involving nine defects in five knees. J Tissue Eng Regen Med 1:74–79.
4. Pittenger MF, AM Mackay, SC Beck, RK Jaiswal, R Douglas, JD Mosca, MA Moorman, DW Simonetti, S Craig and DR Marshak. (1999). Multilineage potential of adult human mesenchymal stem cells. Science 284:143–147.
5. Zuk PA, M Zhu, P Ashjian, DA De Ugarte, JI Huang, H Mizuno, ZC Alfonso, JK Fraser, P Benhaim and MH Hedrick. (2002). Human adipose tissue is a source of multipotent stem cells. Mol Biol Cell 13:4279–4295.
6. Segawa Y, T Muneta, H Makino, A Nimura, T Mochizuki, YJ Ju, Y Ezura, A Umezawa and I Sekiya. (2009). Mesenchymal stem cells derived from synovium, meniscus, anterior cruciate ligament, and articular chondrocytes share similar gene expression profiles. J Orthop Res 27:435–441.
7. Miura M, S Gronthos, M Zhao, B Lu, LW Fisher, PG Robey and S Shi. (2003). SHED: stem cells from human exfoliated deciduous teeth. Proc Natl Acad Sci U S A 100:5807–5812.
8. Gronthos S, M Mankani, J Brahim, PG Robey and S Shi. (2000). Postnatal human dental pulp stem cells (DPSCs) in vitro and in vivo. Proc Natl Acad Sci U S A 97:13625–13630.
9. Stenderup K, J Justesen, C Clausen and M Kassem. (2003). Aging is associated with decreased maximal life span and accelerated senescence of bone marrow stromal cells. Bone 33:919–926.
10. Payne KA, DM Didiano and CR Chu. (2010). Donor sex and age influence the chondrogenic potential of human femoral bone marrow stem cells. Osteoarthritis Cartilage 18:705–713.
11. Takahashi K, K Tanabe, M Ohnuki, M Narita, T Ichisaka, K Tomoda and S Yamanaka. (2007). Induction of pluripotent stem cells from adult human fibroblasts by defined factors. Cell 131:861–872.
12. Yu J, MA Vodyanik, K Smuga-Otto, J Antosiewicz-Bourget, JL Frane, S Tian, J Nie, GA Jonsdottir, V Ruotti, et al. (2007). Induced pluripotent stem cell lines derived from human somatic cells. Science 318:1917–1920.
13. Maherali N, T Ahfeldt, A Rigamonti, J Utikal, C Cowan and K Hochedlinger. (2008). A high-efficiency system for the generation and study of human induced pluripotent stem cells. Cell Stem Cell 3:340–345.
14. Yu J, K Hu, K Smuga-Otto, S Tian, R Stewart, II Slukvin and JA Thomson. (2009). Human induced pluripotent stem cells free of vector and transgene sequences. Science 324:797–801.
15. Jia F, KD Wilson, N Sun, DM Gupta, M Huang, Z Li, NJ Panetta, ZY Chen, RC Robbins, et al. (2010). A nonviral minicircle vector for deriving human iPS cells. Nat Methods 7:197–199.
16. Okita K, Y Matsumura, Y Sato, A Okada, A Morizane, S Okamoto, H Hong, M Nakagawa, K Tanabe, et al. (2011). A more efficient method to generate integration-free human iPS cells. Nat Methods 8:409–412.
17. Johnstone B, TM Hering, AI Caplan, VM Goldberg and JU Yoo. (1998). In vitro chondrogenesis of bone marrow-derived mesenchymal progenitor cells. Exp Cell Res 238: 265–272.
18. Yoo JU, TS Barthel, K Nishimura, L Solchaga, AI Caplan, VM Goldberg and B Johnstone. (1998). The chondrogenic potential of human bone-marrow-derived mesenchymal progenitor cells. J Bone Joint Surg Am 80:1745–1757.
19. Holtzer H, J Abbott, J Lash and S Holtzer. (1960). The loss of phenotypic traits by differentiated cells in vitro, I. Dedifferentiation of cartilage cells. Proc Natl Acad Sci U S A 46:1533–1542.

20. Bigdeli N, C Karlsson, R Strehl, S Concaro, J Hyllner and A Lindahl. (2009). Coculture of human embryonic stem cells and human articular chondrocytes results in significantly altered phenotype and improved chondrogenic differentiation. Stem Cells 27:1812–1821.
21. Sui Y, T Clarke and JS Khillan. (2003). Limb bud progenitor cells induce differentiation of 1pluripotent embryonic stem cells into chondrogenic lineage. Differentiation 71:578–585.
22. Hwang YS, JM Polak and A Mantalaris. (2008). In vitro direct chondrogenesis of murine embryonic stem cells by bypassing embryoid body formation. Stem Cells Dev 17:971–978.
23. Kim JH, HJ Do, HM Yang, JH Oh, SJ Choi, DK Kim, KY Cha and HM Chung. (2005). Overexpression of SOX9 in mouse embryonic stem cells directs the immediate chondrogenic commitment. Exp Mol Med 37:261–268.
24. Vinatier C, D Mrugala, C Jorgensen, J Guicheux and D Noël. (2009). Cartilage engineering: a crucial combination of cells, biomaterials and biofactors. Trends Biotechnol 27:307–314.
25. Medvedev SP, EV Grigor'eva, AI Shevchenko, AA Malakhova, EV Dementyeva, AA Shilov, EA Pokushalov, AM Zaidman, MA Aleksandrova, et al. (2011). Human induced pluripotent stem cells derived from fetal neural stem cells successfully undergo directed differentiation into cartilage. Stem Cells Dev 20:1099–1112.
26. Thomson JA, J Itskovitz-Eldor, SS Shapiro, MA Waknitz, JJ Swiergiel, VS Marshall and JM Jones. (1998). Embryonic stem cell lines derived from human blastocysts. Science 282:1145–1147.
27. Fujioka T, K Yasuchika, Y Nakamura, N Nakatsuji and H Suemori. (2004). A simple and efficient cryopreservation method for primate embryonic stem cells. Int J Dev Biol 48:1149–1154.
28. Koyama N, Y Okubo, K Nakao, K Osawa, K Fujimura and K Bessho. (2011). Pluripotency of mesenchymal cells derived from synovial fluid in patients with temporomandibular joint disorder. Life Sci 89:741–747.
29. Dominici M, K Le Blanc, I Mueller, I Slaper-Cortenbach, F Marini, D Krause, R Deans, A Keating, DJ Prockop and E Horwitz. (2006). Minimal criteria for defining multipotent mesenchymal stromal cells. The International Society for cellular therapy position statement. Cytotherapy 8:315–317.
30. Salem HK and C Thiemermann. (2010). Mesenchymal stromal cells: current understanding and clinical status. Stem Cells 28:585–596.
31. Nishikawa SI, S Nishikawa, M Hirashima, N Matsuyoshi and H Kodama. (1998). Progressive lineage analysis by cell sorting and culture identifies FLK1 + VE-cadherin + cells at a diverging point of endothelial and hemopoietic lineages. Development 125:1747–1757.
32. Simmons PJ and B Torok-Storb. (1991). Identification of stromal cell precursors in human bone marrow by a novel monoclonal antibody, STRO-1. Blood 78:55–62.
33. Ning H, G Lin, TF Lue and CS Lin. (2011). Mesenchymal stem cell marker Stro-1 is a 75 kD endothelial antigen. Biochem Biophys Res Commun 413:353–357.
34. Barberi T, LM Willis, ND Socci and L Studer. (2005). Derivation of multipotent mesenchymal precursors from human embryonic stem cells. PLoS Med 2:e161.
35. Liu Y, AJ Goldberg, JE Dennis, GA Gronowicz and LT Kuhn. (2012). One-step derivation of mesenchymal stem cell (MSC)-like cells from human pluripotent stem cells on a fibrillar collagen coating. PLos One 7:e33225.
36. Wu R, B Gu, X Zhao, Z Tan, L Chen, J Zhu and M Zhang. (2011). Derivation of multipotent nestin(+)/CD271 (-)/STRO-1 (-) mesenchymal-like precursors from human embryonic stem cells in chemically defined conditions. Hum Cell [Epub ahead of print]; DOI:10.1007/s13577-011-0022-3.
37. Honczarenko M, Y Le, M Swierkowski, I Ghiran, AM Glodek and LE Silberstein. (2006). Human bone marrow stromal cells express a distinct set of biologically functional chemokine receptors. Stem Cells 24:1030–1041.
38. Wagner W, P Horn, M Castoldi, A Diehlmann, S Bork, R Saffrich, V Benes, J Blake, S Pfister, V Eckstein and AD Ho. (2008). Replicative senescence of mesenchymal stem cells: a continuous and organized process. PLos One 3:e2213.
39. Jung EM, O Kwon, KS Kwon, YS Cho, SK Rhee, JK Min and DB Oh. (2011). Evidences for correlation between the reduced VCAM-1 expression and hyaluronan synthesis during cellular senescence of human mesenchymal stem cells. Biochem Biophys Res Commun 404:463–469.
40. Toh WS, Z Yang, H Liu, BC Heng, EH Lee and T Cao. (2007). Effects of culture conditions and bone morphogenetic protein 2 on extent of chondrogenesis from human embryonic stem cells. Stem Cells 25:950–960.
41. Nakagawa M, M Koyanagi, K Tanabe, K Takahashi, T Ichisaka, T Aoi, K Okita, Y Mochiduki, N Takizawa and S Yamanaka. (2008). Generation of induced pluripotent stem cells without Myc from mouse and human fibroblasts. Nat Biotechnol 26:101–106.
42. Suemori H, K Yasuchika, K Hasegawa, T Fujioka, N Tsuneyoshi and N Nakatsuji. (2006). Efficient establishment of human embryonic stem cell lines and long-term maintenance with stable karyotype by enzymatic bulk passage. Biochem Biophys Res Commun 345:926–932.
43. Akiyama H, MC Chaboissier, JF Martin, A Schedl and B de Crombrugghe. (2002). The transcription factor Sox9 has essential roles in successive steps of the chondrocyte differentiation pathway and is required for expression of Sox5 and Sox6. Genes Dev 16:2813–2828.
44. Han Y and V Lefebvre. (2008). L-Sox5 and Sox6 drive expression of the aggrecan gene in cartilage by securing binding of Sox9 to a far-upstream enhancer. Mol Cell Biol 28:4999–5013.
45. Lefebvre V and P Smits. (2005). Transcriptional control of chondrocyte fate and differentiation. Birth Defects Res C Embryo Today 75:200–212.
46. Puetzer JL, JN Petitte and EG Loboa. (2010). Comparative review of growth factors for induction of three-dimensional in vitro chondrogenesis in human mesenchymal stem cells isolated from bone marrow and adipose tissue. Tissue Eng Part B Rev 16:435–444.
47. Hwang NS, S Varghese, Z Zhang and J Elisseeff. (2006). Chondrogenic differentiation of human embryonic stem cell-derived cells in arginine-glycine-aspartate-modified hydrogels. Tissue Eng 12:2695–2706.
48. Xu C, J Jiang, V Sottile, J McWhir, J Lebkowski and MK Carpenter. (2004). Immortalized fibroblast-like cells derived from human embryonic stem cells support undifferentiated cell growth. Stem Cells 22:972–980.
49. Lian Q, E Lye, K Suan Yeo, E Khia Way Tan, M Salto-Tellez, TM Liu, N Palanisamy, RM El Oakley, EH Lee, B Lim and SK Lim. (2007). Derivation of clinically compliant MSCs from CD105+, CD24- differentiated human ESCs. Stem Cells 25:425–436.
50. Teramura T, Y Onodera, T Mihara, Y Hosoi, C Hamanishi and K Fukuda. (2010). Induction of mesenchymal progenitor cells with chondrogenic property from mouse-induced pluripotent stem cells. Cell Reprogram 12:249–261.

51. Foster JW, MA Dominguez-Steglich, S Guioli, C Kwok, PA Weller, M Stevanović, J Weissenbach, S Mansour, ID Young, et al. (1994). Campomelic dysplasia and autosomal sex reversal caused by mutations in an SRY-related gene. Nature 372:525–530.
52. Wagner T, J Wirth, J Meyer, B Zabel, M Held, J Zimmer, J Pasantes, FD Bricarelli, J Keutel, et al. (1994). Autosomal sex reversal and campomelic dysplasia are caused by mutations in and around the SRY-related gene SOX9. Cell 79:1111–1120.
53. Bi W, W Huang, DJ Whitworth, JM Deng, Z Zhang, RR Behringer and B de Crombrugghe. (2001). Haploinsufficiency of Sox9 results in defective cartilage primordia and premature skeletal mineralization. Proc Natl Acad Sci U S A 98:6698–6703.
54. Gong G, D Ferrari, CN Dealy and RA Kosher. (2010). Direct and progressive differentiation of human embryonic stem cells into the chondrogenic lineage. J Cell Physiol 224:664–671.
55. Toh WS, XM Guo, AB Choo, K Lu, EH Lee and T Cao. (2009). Differentiation and enrichment of expandable chondrogenic cells from human embryonic stem cells in vitro. J Cell Mol Med 13:3570–3590.
56. Oldershaw RA, MA Baxter, ET Lowe, N Bates, LM Grady, F Soncin, DR Brison, TE Hardingham and SJ Kimber. (2010). Directed differentiation of human embryonic stem cells toward chondrocytes. Nat Biotechnol 28:1187–1194.
57. Lafont JE, S Talma, C Hopfgarten and CL Murphy. (2008). Hypoxia promotes the differentiated human articular chondrocyte phenotype through SOX9-dependent and-independent pathways. J Biol Chem 283:4778–4786.
58. Khan WS, AB Adesida and TE Hardingham. (2007). Hypoxic conditions increase hypoxia-inducible transcription factor 2alpha and enhance chondrogenesis in stem cells from the infrapatellar fat pad of osteoarthritis patients. Arthritis Res Ther 9:R55.
59. Grayson WL, F Zhao, B Bunnell and T Ma. (2007). Hypoxia enhances proliferation and tissue formation of human mesenchymal stem cells. Biochem Biophys Res Commun 358: 948–953.
60. Krinner A, M Zscharnack, A Bader, D Drasdo and J Galle. (2009). Impact of oxygen environment on mesenchymal stem cell expansion and chondrogenic differentiation. Cell Prolif 42:471–484.
61. Feng G, Y Wan, G Balian, CT Laurencin and X Li. (2008). Adenovirus-mediated expression of growth and differentiation factor-5 promotes chondrogenesis of adipose stem cells. Growth Factors 26:132–142.
62. Vinardell T, RA Rolfe, CT Buckley, EG Meyer, M Ahearne, P Murphy and DJ Kelly. (2012). Hydrostatic pressure acts to stabilise a chondrogenic phenotype in porcine joint tissue derived stem cells. Eur Cell Mater 23:121–132.
63. Miura K, Y Okada, T Aoi, A Okada, K Takahashi, K Okita, M Nakagawa, M Koyanagi, K Tanabe, et al. (2009). Variation in the safety of induced pluripotent stem cell lines. Nat Biotechnol 27:743–745.
64. Kulkeaw K, Y Horio, C Mizuochi, M Ogawa and D Sugiyama. (2010). Variation in hematopoietic potential of induced pluripotent stem cell lines. Stem Cell Rev 6:381–389.

Address correspondence to:
Dr. Masako Miura
Department of Medicine and Clinical Science
Kyoto University Graduate School of Medicine
54 Shogoin-Kawaharacho, Sakyo-ku
Kyoto 606-8507
Japan

E-mail: mmiura@kuhp.kyoto-u.ac.jp

Received for publication March 14, 2012
Accepted after revision July 18, 2012
Prepublished on Liebert Instant Online July 20, 2012